Synthesis, Structure, and Dynamic Behavior of Symmetrical *cis*- and *trans*-Alkene Complexes of the Chiral Rhenium Lewis Acid $[(\eta^5\text{-}C_5H_5)Re(NO)(PPh_3)]^+$: Binding Selectivities and Isomerization Processes

Jiaqi Pu, Tang-Sheng Peng, Charles L. Mayne, Atta M. Arif, and J. A. Gladysz*

Department of Chemistry, University of Utah, Salt Lake City, Utah 84112

Received January 22, 1993

Reactions of $[(\eta^5\text{-}C_5H_5)Re(NO)(PPh_3)(ClC_6H_5)]^+BF_4^-$ with *cis*-alkenes (**a**, 2-butene; **b**, 3-hexene; **c**, stilbene; **d**, 1,2-dichloroethylene; −45 °C to room temperature) give the adducts (Z)-$[(\eta^5\text{-}C_5H_5)Re(NO)(PPh_3)(RHC{=}CHR)]^+BF_4^-$ ((Z)-**1a–d**) in 67–95% yields after workup. Reactions with *trans*-alkenes are much slower, and (E)-**1a–c** are isolated in 86–98% yields after 12–24 h at 85–95 °C. Complexes (Z)-**1a–d** are obtained as 70–84:30–16, 85:15, 93:7, and 59:41 equilibrium mixtures of diastereomers that differ by ca. 180° rotations about the Re–(C=C) axes. Variable-temperature and 2D NMR experiments establish rotational barriers of >17.5–11.0 kcal/mol and exclude alternative isomerization pathways. Complexes (E)-**1a–c** are obtained as >99–98:<1–2 equilibrium mixtures of diastereomers that differ in the C=C enantioface bound to rhenium. Kinetic selectivities, obtained from syntheses conducted at 25–60 °C, are lower, although the diastereomers of (E)-**1c** slowly equilibrate in $CDCl_3$ at 25 °C. Complexes (E)-**1a–c** undergo rotation about the Re–(C=C) axes with barriers of 18.6–11.6 kcal/mol. The crystal structures of (Z)-**1a** and (E)-**1a** are determined, and the NMR and dynamic properties of all compounds are analyzed in detail.

Simple achiral alkenes are now frequently utilized as substrates for metal-mediated enantioselective syntheses of organic molecules.[1] In most cases, the alkene initially binds to a chiral metal fragment. This transforms one or both of the C=C carbons into formal stereocenters—a consequence readily envisioned in the Cahn–Ingold–Prelog framework when the complex is drawn in a metallacyclopropane resonance form, as exemplified by structures **A-F** in Scheme I.[2] Thus, over the last five years we have systematically studied the stereochemistry of binding of various classes of alkenes to the chiral rhenium Lewis acid $[(\eta^5\text{-}C_5H_5)Re(NO)(PPh_3)]^+$ (**I**).[3-8]

The rhenium fragment **I** possesses the high-lying d orbital HOMO shown in Scheme I, in which pairs of lobes are directed *syn* and *anti* to the bulky PPh_3 ligand.[9] Alkene ligands adopt Re–(C=C) conformations that allow high degrees of overlap of their π^* acceptor orbitals with this donor orbital, as verified by NMR experiments in solution and several crystal structures.[3a,b,4,6] For the ethylene complex of **I**, the barrier to rotation about the Re–(C=C) axis is 16.4 kcal/mol (96 °C).[3a] In monosubstituted alkene complexes of **I**, Re–(C=C) conformations that place the larger =CHR terminus *anti* to the PPh_3 ligand are greatly preferred.[3]

Monosubstituted alkenes give two configurational diastereomers upon binding to **I**, as illustrated by the idealized structures **II** and **III** in Scheme I.[3] These differ in the C=C enantioface bound to the rhenium. Although kinetic binding selectivities are modest (ca. 2:1), equilibrium can be established at 95–100 °C, and thermodynamic selectivities are high (**II**/**III** ≥96:4 for R = alkyl).[3b] The lower stability of **III** can be attributed to steric interactions between the cyclopentadienyl ligand and the =CHR substituent.

We sought to acquire analogous binding data for *cis* and *trans* disubstituted alkenes. These can also give two configurational diastereomers upon complexation to **I**, although certain differences deserve emphasis. For example, the C=C faces of symmetrical *cis*-alkenes are *homotopic* or identical. Binding to a chiral moiety lifts this degeneracy, giving in the case of **I** the idealized structures **IV** and **V**, which can interconvert by exchange of the ligating C=C faces. However, in contrast to **II** and

(1) This literature is extensive. Some recent references: (a) Coates, G. W.; Waymouth, R. M. *J. Am. Chem. Soc.* **1991**, *113*, 6270. (b) Sharpless, K. B.; Amberg, W.; Beller, M.; Chen, H.; Hartung, J.; Kawanami, Y.; Lübben, D.; Manoury, E.; Ogino, Y.; Shibata, T.; Ukita, T. *J. Org. Chem.* **1991**, *56*, 4585. (c) Noyori, R. *CHEMTECH* **1992**, *12*, 360.

(2) (a) The absolute configuration at rhenium is specified first, and is assigned by a modfication of the Cahn–Ingold–Prelog rules in which the $\eta^5\text{-}C_5H_5$ and RHC=CHR ligands are considered pseudoatoms of atomic numbers 30 and 12, respectively. This gives the priority sequence $\eta^5\text{-}C_5H_5$ > PPh_3 > RHC=CHR > NO. See: (b) Stanley, K.; Baird, M. C. *J. Am. Chem. Soc.* **1975**, *97*, 6598; Sloan, T. E. *Top. Stereochem.* **1981**, *12*, 1; Lecomte, C.; Dusausoy, Y.; Protas, J.; Tirouflet, J.; Dormand, J. *J. Organomet. Chem.* **1974**, *73*, 67. (c) The absolute configurations of the two RHC=CHR stereocenters are given following that of the metal, and are assigned as illustrated by **A–F** in Scheme I (priority sequence Re > CHRRe > CHHRe > R > H; =CHR *anti* to the PPh_3 ligand given first). See: (d) Paiaro, G.; Panunzi, A. *J. Am. Chem. Soc.* **1964**, *88*, 5148. (e) Note that as long as *cis* or *trans* stereochemistry is maintained, the configurations of the RHC=CHR centers are fixed relative to each other.

(3) (a) Bodner, G. S.; Peng, T.-S.; Arif, A. M.; Gladysz, J. A. *Organometallics* **1990**, *9*, 1191. (b) Peng, T.-S.; Arif, A. M.; Gladysz, J. A. *Helv. Chim. Acta* **1992**, *75*, 442. (c) Peng, T.-S.; Gladysz, J. A. *J. Am. Chem. Soc.* **1992**, *114*, 4174.

(4) Kowalczyk, J. J.; Arif, A. M.; Gladysz, J. A. *Chem. Ber.* **1991**, *124*, 729.

(5) Peng, T.-S.; Arif, A. M.; Gladysz, J. A. manuscript in preparation.

(6) Alkene complexes of enones: Wang, Y.; Agbossou, F.; Dalton, D. M.; Liu, Y.; Arif, A. M.; Gladysz, J. A. *Organometallics*, following paper in this issue.

(7) Analogous alkyne complexes: (a) Kowalczyk, J. J.; Arif, A. M.; Gladysz, J. A. *Organometallics* **1991**, *10*, 1079. (b) Ramsden, J. R.; Weng, W.; Gladysz, J. A. *Organometallics* **1992**, *11*, 3635.

(8) Analogous allene complexes: Pu, J.; Peng, T.-S.; Arif, A. M.; Galdysz, J. A. *Organometallics* **1992**, *11*, 3232.

(9) (a) Schilling, B. E. R.; Hoffmann, R.; Faller, J. W. *J. Am. Chem. Soc.* **1979**, *101*, 592. (b) Kiel, W. A.; Lin, G.-Y.; Constable, A. G.; McCormick, F. B.; Strouse, C. E.; Eisenstein, O.; Gladysz, J. A. *J. Am. Chem. Soc.* **1982**, *104*, 4865. (c) Czech, P. T.; Gladysz, J. A.; Fenske, R. F. *Organometallics* **1989**, *8*, 1810.

0276-7333/93/2312-2686$04.00/0

Scheme I. I, d-Orbital HOMO of the Pyramidal 16-Valence-Electron Rhenium Fragment $[(\eta^5\text{-}C_5H_5)Re(NO)(PPh_3)]^+$; II, III, Idealized Structures of Diastereomeric Monosubstituted Alkene Complexes of I; IV, V, Idealized Structures of Diastereomeric *cis*-Alkene Complexes of I; VI, VII, Idealized Structures of Diastereomeric *trans*-Alkene Complexes of I

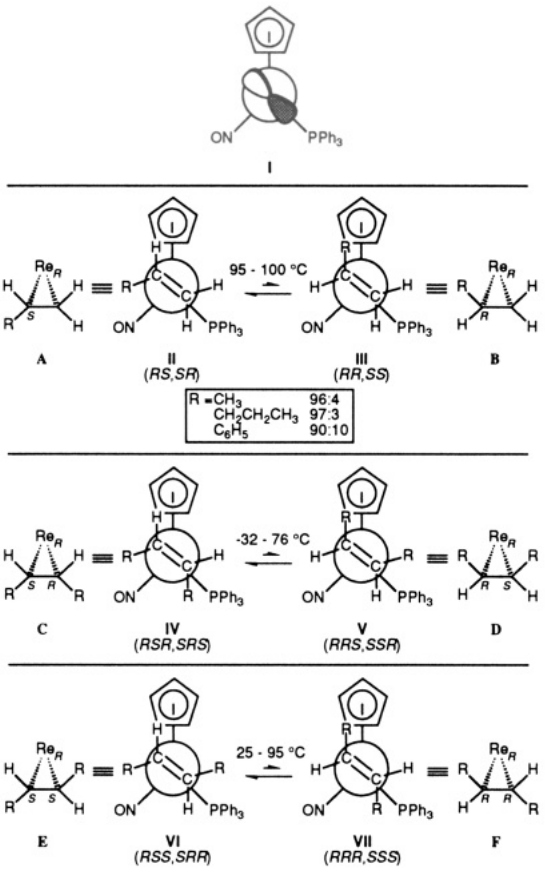

III, **IV** and **V** are also *conformers* that differ by a 180° rotation about the Re–(C=C) axis.

The C=C faces of symmetrical *trans*-alkenes are enantiotopic. Hence, the resulting adducts with **I** (**VI**, **VII**) bear a relationship similar to those encountered with monosubstituted alkenes (**II**, **III**). We thought it likely that, in both *trans*- and *cis*-alkene complexes of **I**, alkyl substituents in either position on the C=C carbon *syn* to the PPh_3 ligand would experience comparable repulsive steric interactions.[10] Thus, we anticipated that the position of the substitutent on the carbon *anti* to the PPh_3 ligand would be the primary determinant of diastereomer stabilities, as with **II** and **III**.

In this paper we report (1) the isolation of a series of acyclic, symmetrical *cis*- and *trans*-alkene complexes of the formula $[(\eta^5\text{-}C_5H_5)Re(NO)(PPh_3)(RHC{=}CHR)]^+BF_4^-$ (**1**), (2) equilibrium data for the binding modes illustrated in Scheme I, (3) energy barriers for the interconversion of diastereomeric *cis*-alkene complexes, and related dynamic processes of *trans*-alkene complexes, and (4) crystal structures of *cis*- and *trans*-2-butene complexes. Complementary studies of analogous *cis*-cycloalkene complexes have been described elsewhere.[4]

Scheme II. Synthesis of Symmetrical *cis*-Alkene Complexes (*Z*)-1

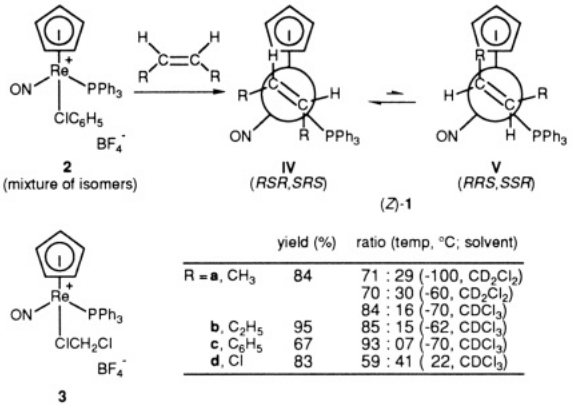

	yield (%)	ratio (temp, °C; solvent)
R = **a**, CH_3	84	71 : 29 (-100, CD_2Cl_2)
		70 : 30 (-60, CD_2Cl_2)
		84 : 16 (-70, $CDCl_3$)
b, C_2H_5	95	85 : 15 (-62, $CDCl_3$)
c, C_6H_5	67	93 : 07 (-70, $CDCl_3$)
d, Cl	83	59 : 41 (22, $CDCl_3$)

Results

1. Synthesis of *cis*-Alkene Complexes. Chlorohydrocarbon complexes of the formula $[(\eta^5\text{-}C_5H_5)Re(NO)(PPh_3)(ClR)]^+BF_4^-$ are substitution-labile and serve as convenient functional equivalents of the chiral Lewis acid **I**.[11,12] Thus, the chlorobenzene complex $[(\eta^5\text{-}C_5H_5)Re(NO)(PPh_3)(ClC_6H_5)]^+BF_4^-$ (**2**) was generated in C_6H_5Cl at −45 °C as described earlier.[11] In separate experiments, excesses of (**a**) *cis*-2-butene, (**b**) *cis*-3-hexene, (**c**) *cis*-stilbene, or (**d**) *cis*-1,2-dichloroethylene were added. After 5–24 h at room temperature, workup gave the corresponding *cis*-alkene complexes (*Z*)-$[(\eta^5\text{-}C_5H_5)Re(NO)(PPh_3)(RHC{=}CHR)]^+BF_4^-$ ((*Z*)-**1a–d**) in 67–95% yields (Scheme II).

A similar reaction of dichloromethane complex $[(\eta^5\text{-}C_5H_5)Re(NO)(PPh_3)(ClCH_2Cl)]^+BF_4^-$ (**3**)[12] and *cis*-2-butene also gave (*Z*)-**1a** (87%). However, **3** has usually been found to be less reactive than **2**, and gave much poorer results with other disubstituted alkenes. Reactions of **2** with *cis*-3-hexene and *cis*-1,2-dichloroethylene were monitored by ^{31}P NMR spectroscopy. The former was complete within 4 h at −45 °C, but the latter required 24 h at room temperature.

Complexes (*Z*)-**1a–d**, and other new alkene complexes described below, were characterized by microanalysis and IR and NMR (^1H, ^{13}C, ^{31}P) spectroscopy (Experimental Section). Most properties were similar to those previously reported for monosubstituted and cyclic alkene complexes of **I**. The IR ν_{NO} value of (*Z*)-**1d** (1755 cm^{-1}) was greater than those of (*Z*)-**1a–c** (1716–1722 cm^{-1}), reflecting the greater π acidity (and diminished basicity)[13] of the dichloroethylene ligand, and a concomitant decrease in back-bonding to the nitrosyl ligand.

In each case, NMR spectra at sufficiently low temperature revealed the presence of two diastereomers. The diastereomer ratios increased from 59:41 to 93:7[14] as the size of the C=C substituents increased (Cl < CH_3 < C_2H_5 < C_6H_5; Scheme II). In accord with the stability expectations outlined in the introduction, these were assigned as *RSR,SRS* (**IV**, major) and *RRS,SSR* (**V**, minor)

(10) However, the interstice between the PPh_3 and nitrosyl ligand is more congested than that between the PPh_3 and cyclopentadienyl ligand: (a) Crocco, G. L.; Lee, K. E.; Gladysz, J. A. *Organometallics* **1990**, *9*, 2819. (b) Davies, S. G.; Dordor-Hedgecock, I. M.; Sutton, K. H.; Whittaker, M. *J. Am. Chem. Soc.* **1987**, *109*, 5711. (c) Mackie, S. C.; Baird, M. C. *Organometallics* **1992**, *11*, 3712. (d) Polowin, J.; Mackie, S. C.; Baird, M. C. *Organometallics* **1992**, *11*, 3724.

(11) Kowalczyk, J. J.; Agbossou, S. K.; Gladysz, J. A. *J. Organomet. Chem.* **1990**, *397*, 333.

(12) Fernández, J. M.; Gladysz, J. A. *Organometallics* **1989**, *8*, 207.

(13) Bursten, B. E.; Green, M. R. *Prog. Inorg. Chem.* **1988**, *36*, 393.

(14) All isomer ratios are normalized to 100, and error limits on each integer are ±2; e.g., 59:41 ≡ 59 ± 2:41 ± 2.

Scheme III. Synthesis of Symmetrical *trans*-Alkene Complexes (*E*)-1

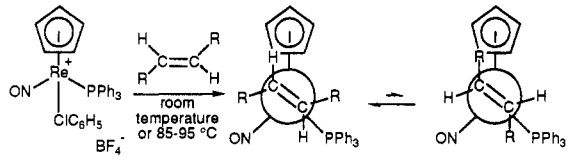

	(*E*)-1 ratio	
	room temperature	85-95 °C (yield, %)
R = **a**, CH_3	89 : 11	99 : 1 (92)
b, C_2H_5	--	>99 : 1 (86)
c, C_6H_5	76 : 24	98 : 2 (98)

diastereomers, respectively. Further support for these structures is given below. The *cis*-2-butene complex (*Z*)-**1a** gave slightly different diastereomer ratios in $CDCl_3$ and CD_2Cl_2. This was reproduced under a variety of conditions utilizing integrals of different ^1H and ^{31}P NMR resonances. Since the *cis*-1,2-dichloroethylene complex (*Z*)-**1d** gave a diastereomer ratio close to unity, ^{31}P and C=C ^{13}C NMR resonance assignments were verified by heteronuclear decoupling experiments (supplementary material).

2. Synthesis of *trans*-Alkene Complexes. The chlorobenzene complex **2** and symmetrical *trans*-alkenes were reacted as summarized in Scheme III. However, substitution was much slower than with *cis*-alkenes. For example, the reaction of **2** and a large excess of *trans*-2-butene required 6 days at room temperature. Workup gave a 77:10:13 mixture of the *RSS,SRR* and *RRR,SSS* diastereomers of (*E*)-**1a** (**VI, VII**) and the *cis*-2-butene complex (*Z*)-**1a** (87% total). Diastereomer assignments were based upon the NMR and stability properties described below. The (*Z*)-**1a** was assumed to arise from trace quantities of *cis*-2-butene in the *trans*-2-butene, although none could be detected by ^1H NMR. However, in view of the excess alkene employed, the greater nucleophilicity of *cis*-2-butene could lead to a disproportionate amount of product.[15]

Next, **2** and *trans*-3-hexene were combined in a NMR tube. After 10 days at room temperature, only a very small amount of the corresponding complex (*E*)-**1b** was present, as assayed by ^{31}P NMR. A sample that was kept for a brief period at 60 °C showed ca. 25% conversion to a 52:48 mixture of *RSS,SRR/RRR,SSS* diastereomers (7.5, 7.0 ppm). However, reaction of **2** and *trans*-stilbene was complete within 24 h at room temperature. Workup of a preparative experiment gave (*E*)-**1c** as a 76:24 mixture of *RSS,SRR/RRR,SSS* diastereomers (53%). In all cases, no *cis* isomers were detected.

As noted above, diastereomers of analogous monosubstituted alkene complexes interconvert at 95 °C (**II/III**, Scheme I). Thus, in order to both reduce reaction times and directly access equilibrium mixtures of diastereomers, samples of **2** and *trans*-2-butene, *trans*-3-hexene, and *trans*-stilbene were kept at 85–95 °C for 12–20 h. Workup gave (*E*)-**1a–c** in 86–98% yields as >99–98:<1–2 mixtures of *RSS,SRR/RRR,SSS* diastereomers (Scheme III).[16] However, under identical conditions *trans*-1,2-dichloroethylene gave, in addition to a spectroscopically detectable quantity of (*E*)-**1d**, a multitude of byproducts. The IR ν_{NO} values of (*E*)-**1a–c** were consistently 3–10 cm^{-1} greater than those of (*Z*)-**1a–c**, and NMR data are analyzed below.

Chart I. Summary of ^1H Difference NOE Enhancements for Alkene Complexes (from Cyclopentadienyl Ligand Irradiation)

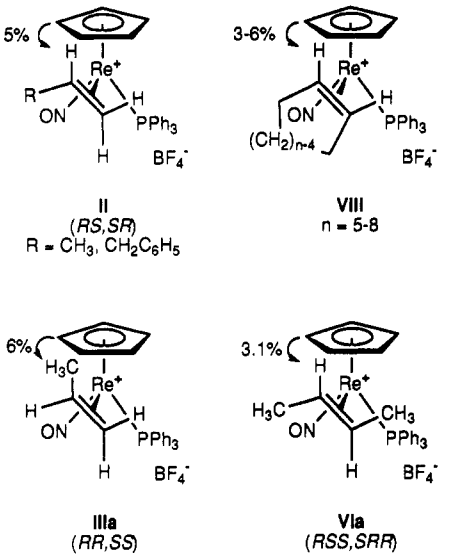

II (*RS,SR*) R = CH_3, $CH_2C_6H_5$ — **VIII** n = 5-8

IIIa (*RR,SS*) — **VIa** (*RSS,SRR*)

A sample of *trans*-stilbene complex (*E*)-**1c** that had been prepared at room temperature was chromatographed. One series of fractions was enriched in the less stable diastereomer (11:89 *RSS,SRR/RRR,SSS*). This mixture was dissolved in $CDCl_3$ and kept at room temperature. After 2 days, the *RSS,SRR/RRR,SSS* diastereomer ratio had changed to 56:44. Thus, isomerization of the less stable diastereomer of (*E*)-**1c** is much more rapid than that of the corresponding styrene complex.[3c]

3. NMR Properties of Complexes. The NMR properties of monosubstituted and *cis*-cycloalkene complexes of **I** have been studied in detail.[3,4] The ^1H NMR resonances of groups that are *syn* to the cyclopentadienyl ligand on the C=C carbon *anti* to the PPh_3 ligand can be assigned by difference NOE experiments,[17] as illustrated for **II**, **VIII**, and **IIIa** in Chart I. In the *cis* complexes **VIII**, the =CH protons on the C=C carbons *syn* to the PPh_3 ligand were shown to be upfield of those on the C=C carbons *anti* to the PPh_3 ligand. Hence, analogous assignments were made for the *RSR,SRS* diastereomers of *cis* complexes (*Z*)-**1a–d**, and in coalesced spectra in which these diastereomers provided the dominant contribution. For the phenyl and chloride substituted complexes (*Z*)-**1c,d**, all =CH ^1H NMR couplings were resolved. Importantly, the =CH protons *syn* to the PPh_3 ligand gave large J_{HP} (11.6–13.7 Hz), but those *anti* to the PPh_3 ligand gave small J_{HP} (≤1.5 Hz).

The C=C ^{13}C NMR resonances of alkene complexes of **I** exhibit differing $^2J_{CP}$ values.[3,4] That of the carbon *syn* to the PPh_3 ligand is typically 4–6 Hz, whereas the other is <2 Hz. In room temperature ^{13}C NMR spectra of (*Z*)-

(15) Many studies have shown that K_{eq} for the formation of *cis*-2-butene complexes is greater than that for the formation of *trans*-2-butene complexes: Herberhold, M. *Metal π-Complexes*; Elsevier: New York, 1974; Vol. II, Part 2, Chapter VIII. To our knowledge quantitative nucleophilicity comparisons are scarce, although the qualitative ordering *cis* > *trans* seems assured from a variety of competition experiments that have appeared in the literature.

(16) Separate NMR experiments established that diastereomer ratios were unaffected by workup, and that no independent thermal decomposition occurred.

(17) Neuhaus, D.; Williamson, M. *The Nuclear Overhauser Effect in Structural and Conformational Analyses*; VCH: New York, 1989; Chapter 7.

Chart II. Methyl Resonance ^1H NMR Chemical Shift Trends in Propene and Butene Complexes[a]

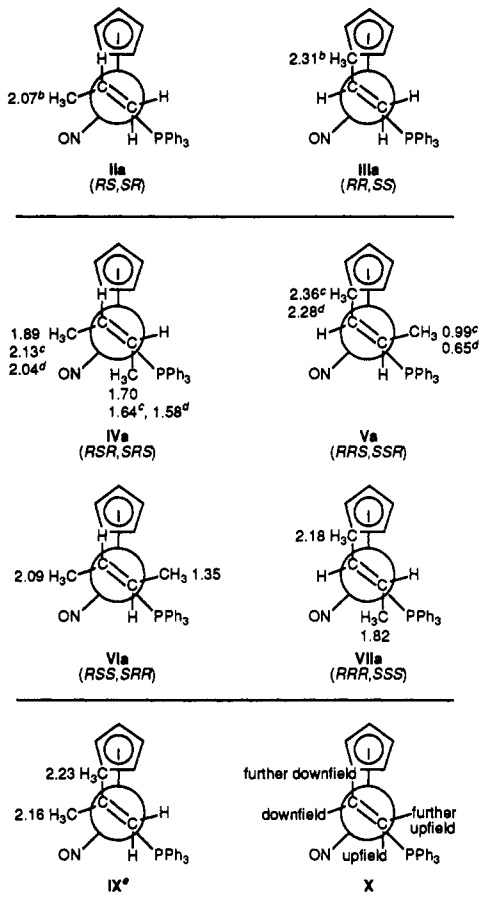

[a] In $CDCl_3$ and ambient probe temperature unless noted. [b] See ref 3a for chemical shifts in CD_2Cl_2. [c] At −74 °C. [d] In CD_2Cl_2 at −100 °C. [e] In CD_2Cl_2; see ref 18.

1a–c, the downfield C=C resonances (53.4–59.0 ppm) were either doublets or much broader than the upfield resonances (50.4–55.7 ppm), which were singlets. For both the *RSR,SRS* and *RRS,SSR* diastereomers of *cis*-1,2-dichloroethylene complex (*Z*)-**1d**, the downfield C=C resonances were doublets (56.0, 58.3 ppm; J_{CP} = 7.9, 8.8 Hz), and the upfield resonances were again singlets (54.9, 49.6 ppm). Thus, the downfield C=C resonances were assigned to the carbons *syn* to the PPh_3 ligand.

As a check on these =CH group ^1H and ^{13}C NMR shielding trends, the *down*field =CH ^1H resonances of *both* diastereomers of (*Z*)-**1d** were irradiated (δ 5.50, 6.10; supplementary material). In each case, the *up*field =CH ^{13}C resonance was decoupled (54.9, 49.5 ppm). Similarly, irradiation of the upfield =CH ^1H resonances decoupled the downfield =CH ^{13}C resonance. Significantly, this suggests that the =CH ^1H and ^{13}C NMR shielding trends also hold for the *RRS,SSR* series of diastereomers.

Next, the =CH ^1H NMR resonances of *cis*-2-butene complex (*Z*)-**1a** were irradiated (supplementary material). This allowed *syn* and *anti* methyl ^1H resonances to be assigned as shown in **IVa**, Chart II. Then ^{13}C NMR spectra were recorded while the methyl ^1H resonances were irradiated. These showed the upfield and downfield methyl groups (16.2, 18.3 ppm) to be on the C=C carbons *syn* and *anti* to the PPh_3 ligand, respectively. Thus, the *syn/anti*-methyl groups exhibit parallel ^1H and ^{13}C NMR shielding trends, in contrast to the =CH groups.

Analogous data were sought for *trans*-alkene complexes (*E*)-**1a–c**. First, a difference NOE experiment was conducted with the *RSS,SRR* diastereomer of *trans*-2-butene complex (*E*)-**1a**. Irradiation of the cyclopentadienyl ^1H NMR resonance gave a 3.1% enhancement in the downfield =CH ^1H resonance (δ 4.50), but none in the upfield resonance (δ 3.08). Hence, the former was assigned to the =CH proton *anti* to the PPh_3 ligand, as indicated in **VIa** (Chart I). The =CH ^1H NMR resonances of the *RSS,SRR* diastereomers of *trans*-3-hexene and *trans*-stilbene complexes (*E*)-**1b,c** were assigned similarly. No NOE enhancements were observed in either methyl resonance (compare **IIIa**, Chart I).

The *RSS,SRR* diastereomers of *trans*-2-butene and *trans*-stilbene complexes (*E*)-**1a,c** exhibited resolved =CH ^1H NMR couplings. The downfield =CH ^1H NMR resonances gave smaller J_{HP} (≤1.7 Hz) than the upfield =CH resonances (5.4–7.6 Hz), consistent with the NOE result. The downfield C=C ^{13}C NMR resonances of (*E*)-**1a–c** (56.2–61.8 ppm) were either doublets (J_{CP} = 5.3–3.1 Hz) or much broader than the upfield resonances (50.2–56.3 ppm, s). Hence, they were attributed to the carbons *syn* to the PPh_3 ligand.

Decoupling experiments with the *RSS,SRR* diastereomer of *trans*-2-butene complex (*E*)-**1a** (supplementary material) allowed *syn*- and *anti*-methyl ^1H NMR resonances to be assigned as shown in **VIa** (Chart II). Then ^{13}C NMR spectra were recorded while the methyl ^1H resonances were irradiated. These showed the upfield and downfield methyl groups (22.4, 23.9 ppm) to be on the C=C carbons *syn* and *anti* to the PPh_3 ligand, respectively. Thus, the *syn/anti*-methyl groups exhibit parallel ^1H and ^{13}C NMR shielding trends, as found for (*Z*)-**1a**.

As a result of the small quantities produced, only partial NMR data were obtained for the *RRR,SSS* diastereomers of *trans*-2-butene and *trans*-3-hexene complexes (*E*)-**1a,b**. For the former, methyl group ^1H NMR resonances were assigned as depicted in **VIIa** (Chart II). This gave the best match with the methyl group shielding patterns exhibited by the *RSR,SRS* diastereomer of (*Z*)-**1a**, the *RSS,SRR* diastereomer of (*E*)-**1a**, and related propene and isobutene complexes (**IIa**, **IIIa**, **IX**; Chart II).[3a,18] Complete NMR data were acquired for the *RRR,SSS* diastereomer of *trans*-stilbene complex (*E*)-**1c**. As in all of the above compounds, the downfield C=C ^{13}C resonance (54.2 ppm) gave a larger J_{CP} (5.4 Hz) than the upfield resonance (50.5 ppm, s), and the upfield =CH ^1H resonance (δ 4.21) gave a larger J_{HP} (7.8 Hz) than the downfield resonance (δ 5.38, s). Hence, these were assigned to the =CH group *syn* to the PPh_3 ligand.

Due to the small equilibrium concentrations present, only partial NMR data were obtained for the *RRS,SSR* diastereomers of (*Z*)-**1a–c**. For the *cis*-2-butene complex (*Z*)-**1a**, methyl group ^1H resonances were assigned as shown in **Va** (Chart II). Many other trends were apparent in the NMR properties of (*Z*)- and (*E*)-**1**. For example, the ^{31}P resonances of the *RRS,SSR* diastereomers of (*Z*)-**1a,c,d** (10.8, 5.8, 6.9 ppm) were downfield of those of the *RSR,SRS* diastereomers (8.2, 3.7, 6.4 ppm). Similarly, the ^{31}P resonances of the *RSS,SRR* diastereomers of (*E*)-**1a–c** (7.7, 7.5, 5.4 ppm) were downfield of those of the *RRR,SSS* diastereomers (7.1, 7.1, 4.0 ppm).

(18) Roger, C.; Bodner, G. S.; Hatton, W. G.; Gladysz, J. A. *Organometallics* **1991**, *10*, 3266.

Scheme IV. Possible Pathways for the Interconversion of Diastereomers of *cis*-2-Butene Complex (*Z*)-1a

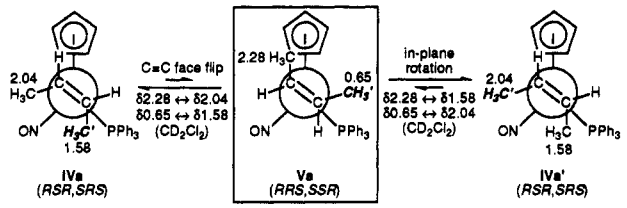

4. Variable Temperature NMR of *cis*-2-Butene Complex (*Z*)-1a. The NMR resonances of the two diastereomers of *cis*-alkene complexes (*Z*)-1a–c coalesced below room temperature, indicating facile equilibration. Importantly, the four sets of =CHR ^{1}H and ^{13}C resonances in the low temperature limit collapsed to *two* in the high-temperature limit. Interconversion by alkene dissociation would simultaneously equivalence all =CHR resonances.

Two distinct nondissociative pathways can be envisioned, as diagramed for the *cis*-2-butene complex (*Z*)-1a in Scheme IV. These require either an in-plane rotation about the Re–(C=C) axis, or a C=C "face flip" in which the rhenium somehow transverses through the π nodal plane. The former, which has abundant precedent, coalesces the upfield methyl resonance of one diastereomer and the downfield resonance of the other. The latter, which has precedent in this series of compounds,[3c] coalesces the upfield methyl resonance of one diastereomer and the upfield resonance of the other.

Hence, variable-temperature ^{1}H NMR spectra of (*Z*)-1a were recorded in CD_2Cl_2 and $CDCl_3$, as shown in Figures 1 and 2. However, pairs of coalescing methyl resonances were difficult to assign from 1D spectra due to broadening and the possibility of temperature-dependent chemical shifts. Furthermore, at the high temperature limit, two methyl resonances were observed in $CDCl_3$, but only one in CD_2Cl_2.

We sought to unambiguously assign the coalescing peaks by 2D NMR exchange experiments.[19,20] First, spectra were acquired in CD_2Cl_2 at −95 °C (178 K). No off-diagonal resonances were observed, indicating no exchange or cross relaxation between any pair of methyl groups. Thus, the absence of cross relaxation can also be safely assumed at higher temperatures. Analogous spectra were recorded at −60 °C (213 K), at which temperature the methyl resonances in the 1D spectra were broadened and the δ 0.65 resonance shifted to δ 0.80. Off-diagonal peaks indicative of methyl group exchange were now found, as shown in the bottom spectrum in Figure 1.

Importantly, the off-diagonal peaks occurred only on the intercepts of the δ 2.04/0.80 and 1.58/2.28 methyl resonances. As analyzed above, this indicates that the (*Z*)-1a diastereomers preferentially equilibrate by rotation about the Re–(C=C) axis.[21] Analogous spectra were acquired with longer mixing times (−60 °C, 0.010–1.000 s).

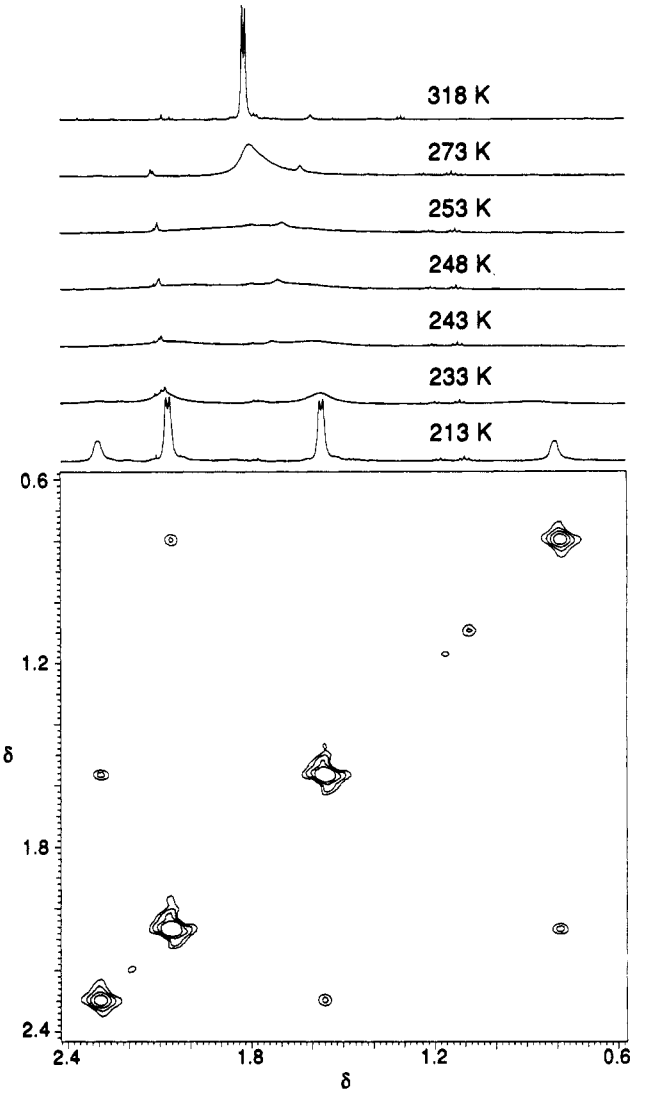

Figure 1. ^{1}H NMR spectra of (*Z*)-1a in CD_2Cl_2: top, 1D spectra at several temperatures; bottom, chemical exchange map (mixing time 0.005 s, 213 K).

No additional off-diagonal peaks were observed. Standard analysis using the initial slope approximation gave rate constants for the exchange of each pair of methyl groups (δ 2.04/0.80: $k_1 = 16.4 \pm 3.1\ s^{-1}$, $k_{-1} = 6.34 \pm 1.20\ s^{-1}$; δ 1.58/2.28: $k_1 = 15.8 \pm 2.7\ s^{-1}$, $k_{-1} = 7.28 \pm 1.25\ s^{-1}$).[22] These gave the $\Delta G^{\ddagger}$ summarized in Table I (11.1–11.5 kcal/mol).

Using the relationships established by the 2D NMR spectra, $\Delta G^{\ddagger}$ were also calculated from the 1D NMR spectra in Figure 2.[23a] These agreed with the values from the 2D NMR experiments, as well as those obtained from the ^{31}P NMR PPh_3 resonances (8.20/10.77 ppm), which coalesced at −27 °C or 246 K (Table I). Although the uncertainties in coalescence temperatures in Figure 2 were greater than normal (±5 °C), they translated into relatively small error limits. From the frequency difference between the two methyl resonances in the high temperature limit, a lower bound of 16.3 kcal/mol (60 °C or 333 K) was calculated for the $\Delta G^{\ddagger}$ of any process capable of effecting

(19) Ernst, R. R.; Bodenhausen, G.; Wokaun, A. *Principles of Nuclear Magnetic Resonance in One and Two Dimensions*; Clarendon: Oxford, 1987; Chapter 9.

(20) (a) Huang, Y.; Macura, S.; Ernst, R. R. *J. Am. Chem. Soc.* **1981**, *103*, 5328. (b) DiMeglio, C. M.; Ahmed, K. J.; Luck, L. A.; Weltin, E. E.; Rheingold, A. L.; Bushweller, C. H. *J. Phys. Chem.* **1992**, *96*, 8765.

(21) A recent solid-state ^{13}C NMR study of ethylene absorbed on a silver surface has also established that rotation about the M – (C=C) axis has a lower energy barrier than a C=C "face flip". However, both dynamic processes occur rapidly at room temperature: Wang, J.; Ellis, P. D. *J. Am. Chem. Soc.* **1993**, *115*, 212.

(22) Rate constants were determined from the slopes of plots of normalized cross-peak volumes ($I_{kl}(\tau_m)/M_{kl}$) vs mixing times (τ_m; 0.005, 0.010, 0.020 s), and are represented with 95% confidence limits as calculated by the program Statview (Abacus Concepts, Inc., Berkeley, CA, 1992). Standard deviations are ±1.1, 0.43, 1.0, and 0.45 s^{-1}, respectively. See ref 19, pp 500–501.

(23) Sandström, J. *Dynamic NMR Spectrometry*; Academic Press: New York, 1982 (a) Chapter 7; (b) pp 53–59.

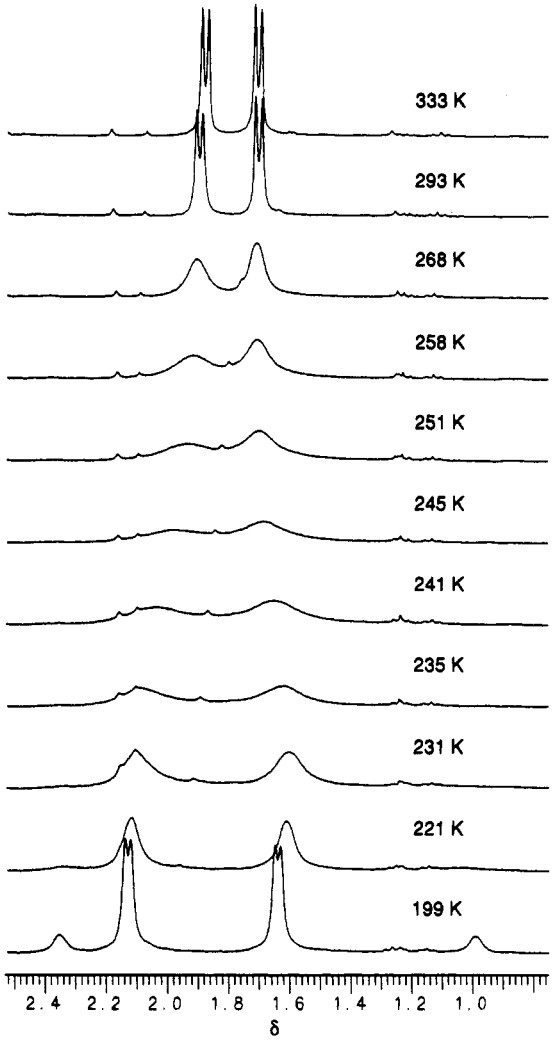

Figure 2. ^1H NMR spectra of (*Z*)-**1a** in $CDCl_3$ at several temperatures.

further methyl group exchange. Apparently, the chemical shifts of the coalesced pairs of methyl resonances are accidentally degenerate in the high-temperature limit in Figure 1.[24]

5. Variable Temperature NMR of Other Complexes. The dynamic NMR properties of the other *cis*-alkene complexes were examined. The methyl ^1H resonances of the diastereomers of *cis*-3-hexene complex (*Z*)-**1b** coalesced at −2.9 °C or 270 K (δ 1.24/0.88) and 0.7 °C or 274 K (δ 0.60/1.35) in $CDCl_3$. These data gave $\Delta G^{\ddagger}$ of 12.8–12.6 kcal/mol (270–274 K) for the conversion of the less stable *RRS,SSR* diastereomer to the more stable *RSR,SRS* diastereomer, as summarized in Table I. The cyclopentadienyl ^1H resonances of the diastereomers of *cis*-stilbene complex (*Z*)-**1c** coalesced at 7.0 °C or 280 K in $CDCl_3$. This gave a $\Delta G^{\ddagger}$ of 13.2 kcal/mol (280 K) for the conversion of the *RRS,SSR* to the *RSR,SRS* diastereomer (Table I).

The diastereomers of *cis*-1,2-dichloroethylene complex (*Z*)-**1d** exhibited distinct sets of NMR resonances at room temperature. We sought to establish whether they also readily interconverted. This would allow the 59:41 ratio in Scheme I to be represented as an equilibrium constant. Accordingly, when the δ 5.50 =CH ^1H NMR resonance of the *RSR,SRS* diastereomer was irradiated, the intensity of the δ 5.04 =CH ^1H resonance of the *RRS,SSR* diastereomer diminished (supplementary material). Irradiation of the other three =CH ^1H NMR resonances gave analogous behavior. Patterns were consistent with saturation transfer[23b] between diastereomers via rotation about the Re–(C=C) axis. Also, the PPh_3 ^{31}P NMR resonances of the diastereomers broadened and began to coalesce in C_6D_5Cl at 76 °C or 349 K. However, partial decomposition occurred, and accelerated at higher temperatures (ca. 50%, 90 °C). These data bounded the $\Delta G^{\ddagger}$ for diastereomer interconversion as ≥17.5 kcal/mol (349 K).

In complexes of **I** and symmetrical *trans*-alkenes, rotation about the Re–(C=C) axis equivalences the =CHR substituents, as diagramed in Scheme V. Accordingly, the methyl ^1H NMR resonances of the *RSS,SRR* diastereomer of *trans*-2-butene complex (*E*)-**1a** coalesced at 124 °C or 397 K in C_6D_5Cl. This gave a $\Delta G^{\ddagger}$ of 18.6 kcal/mol (397 K) for methyl group exchange (Table I). Importantly, partial decomposition occurred near the coalescence temperature to give some free *trans*-2-butene (δ 1.65 d, J = 4.7 Hz, CH_3). Since the bound *trans*-2-butene gave a distinct resonance (δ 1.81 br d), a dissociative exchange mechanism can be excluded. Similar results were obtained in $CDCl_2CDCl_2$. Further heating to 155 °C gave complete decomposition without additional coalescence.

The *RSS,SRR* diastereomer of *trans*-stilbene complex (*E*)-**1c** exhibited two =CH ^1H and ^{13}C NMR resonances, and eight C*Ph* ^{13}C resonances, at room temperature. The =CH ^1H resonances broadened and began to coalesce at 120 °C or 393 K in C_6D_5Cl. However, complete decomposition occurred at 135 °C. Thus, $\Delta G^{\ddagger}$ for rotation about the Re–(C=C) axis is at least 17.6 kcal/mol (393 K). The *RRR,SSS* diastereomer of (*E*)-**1c** gave only one =CH ^1H and ^{13}C NMR resonance, and four C*Ph* ^{13}C resonances, at room temperature. However, the number of resonances doubled at −70 °C. The =CH ^1H resonances coalesced at −15 °C or 258 K in $CDCl_3$, giving a $\Delta G^{\ddagger}$ of 11.6 kcal/mol (258 K) for Re–(C=C) rotation (Table I).

6. Crystal Structures of *cis*- and *trans*-2-Butene Complexes 1a. X-ray data were collected on solvates of (*Z*)-**1a** and the *RSS,SRR* diastereomer of (*E*)-**1a** as outlined in Table II. Refinement gave the structures shown in Figures 3 and 4. The butene ligand =CH hydrogens were located. Atomic coordinates, and selected bond lengths, bond angles, and torsion angles, are summarized in Tables III and IV.

Figure 3 shows that (*Z*)-**1a** crystallizes as a *RSR,SRS* diastereomer, consistent with the major isomer present in solution, and adopts a Re–(C=C) conformation close to that of idealized rotamer **IV**. In **IV**, the $\overline{Re\text{–}C{=}C}$ plane defines angles of 0° and ±90°, respectively, with the Re–P and Re–N bonds. In (*Z*)-**1a**, the corresponding angles were 12.3° and 69.5°. The angle of the $\overline{Re\text{–}C{=}C}$ plane with that defined by the cyclopentadienyl centroid, rhenium, and C=C centroid also provides a measure of alkene ligand conformation. This angle is 45° in **IV**, and was calculated to be 64.2° in (*Z*)-**1a**.

The alkene substituents in (*Z*)-**1a** were markedly bent out of the π nodal plane of the free alkene. In order to quantify this feature, a plane was defined that contained the C=C carbons (C1, C2) but was perpendicular to the $\overline{Re\text{–}C{=}C}$ plane. The angles of the C1–H1, C1–C4, C2–H2, and C2–C3 bonds with this plane were 36.2°, 25.7°,

(24) As an additional check, a 2D NMR spectrum was acquired at −35 °C. The methyl resonances of the *RSR,SRS* diastereomer were broadened, but no off-diagonal peak indicative of independent exchange was detected.

Table I. Summary of Dynamic NMR Data for Diastereomeric Symmetrical Alkene Complexes $[(\eta^5\text{-}C_5H_5)Re(NO)(PPh_3)(RHC{=}CHR)]^+BF_4^-$ (1)

compd	solvent	coalescing resonances (chemical shift, ppm)	$\Delta\nu$, Hz (T, K)[a]	T_c, K	ΔP[b]	$\Delta G^{\ddagger}$,[c] kcal/mol
(*Z*)-**1a**	$CDCl_3$	^1H CH_3 (1.64/2.36)[d]	214.7 (199)	241	0.688	11.1 ± 0.2 11.8 ● 0.2[e]
		^1H CH_3' (2.13/0.99)[d]	276.7 (199)	245	0.678	11.0 ± 0.2 11.7 ± 0.2[e]
		^1H CH_3'' (1.90/1.70)	58.2 (293)	>333	<0.02	>16.3[f]
	CD_2Cl_2	^{31}P PPh_3 (8.20/10.77)[d]	311.1 (173)	246	0.372	11.1 ± 0.1 11.4 ± 0.1[e]
	CD_2Cl_2[g]	^1H CH_3 (1.58/2.28)[d]				11.1 11.5[e]
		^1H CH_3' (2.04/0.80)[d]				11.1 11.5[e]
(*Z*)-**1b**	$CDCl_3$	^1H CH_3 (1.24/0.88)[d]	108.9 (211)	270	0.700	12.8 ± 0.1 13.5 ± 0.1[e]
		^1H CH_3' (0.60/1.35)[d]	224.4 (211)	274	0.700	12.6 ● 0.1 13.3 ± 0.1[e]
(*Z*)-**1c**	$CDCl_3$	^1H C_5H_5 (6.01/5.55)[d]	138.5 (203)	280	0.869	13.2 ± 0.1 14.3 ± 0.1[e]
(*Z*)-**1d**	C_6D_5Cl	^{31}P PPh_3 (6.40/6.71)[d]	37.8 (283)	>349[h]	0.070	>17.5
(*E*)-**1a** (*RSS,SRR*)	C_6D_5Cl	^1H CH_3 (2.10/1.41)	207.8 (298)	397[h]	<0.02	18.6 ± 0.1
(*E*)-**1c** (*RSS,SRR*)	C_6D_5Cl	^1H =CH (6.44/4.51)	576.9 (298)	>393[h]	<0.02	>17.6
(*E*)-**1c** (*RRR,SSS*)	$CDCl_3$	^1H =CH (5.38/4.21)	354.0 (203)	258	<0.02	11.6 ± 0.1

[a] Frequency difference at the low temperature limit (T) for the two resonances that coalesce at T_c. [b] $\Delta P = P_1 - P_2$, where P_1 and P_2 are normalized areas of the two coalescing resonances, as determined by integration of the low-temperature-limit spectrum. [c] At T_c; error limits correspond to an uncertainty of ±2 K in T_c, except with the ^1H data for (*Z*)-**1a** in $CDCl_3$ (±5 K); see ref 23a. [d] Major (*RSR,SRS*) diastereomer/minor (*RRS,SSR*) diastereomer. [e] For the conversion of the major diastereomer to the minor diastereomer. [f] Lower bound for any process that can exchange the two coalesced CH_3 and CH_3' resonances. [g] Data from 2D NMR exchange experiments (213 K). [h] Some decomposition occurs at this temperature.

Scheme V. Possible Degenerate and Nondegenerate Isomerizations of Symmetrical *trans*-Alkene Complex (*E*)-1

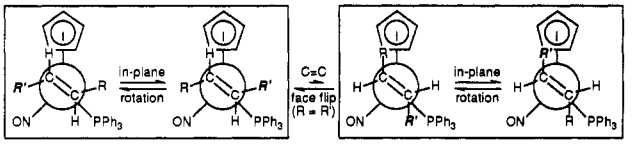

VI (*RSS,SRR*) VII (*RRR,SSS*)

13.8°, and 19.3°, respectively. These would be 0° in an idealized sp^2 hybridized alkene. The C—C1⋯C2—H torsion angles (136°, −120°) also differed from that of the free alkene (180°). In this context, the informative but derivationally more complex α, β, and β' angles utilized by Ibers were also calculated (89.5°, 51.7°, 36.3°).[25]

Figure 4 shows that the *RSS,SRR* diastereomer of (*E*)-**1a** adopts a Re–(C⋯C) conformation similar to that of idealized rotamer **VI**. The Re–C⋯C plane gave angles of 22.6°, 66.4°, and 71.8°, respectively, with the Re–P bond, Re–N bond, and the plane defined by the cyclopentadienyl centroid, rhenium, and C⋯C centroid. The alkene substituents in (*E*)-**1a** were also markedly bent out of the π nodal plane of the free alkene. A plane was again defined that contained C1 and C2 but was perpendicular to the Re–C⋯C plane. The angles of the C1–H1, C1–C4, C2–H2, and C2–C3 bonds with this plane were 25.0°, 18.2°, 19.5°, and 16.8°, respectively. The C4–C1–C2–C3 torsion angle (−139°) also differed greatly from that of the free alkene (180°), and the Ibers α, β, and β' angles were calculated (71.9°, 51.3°, 57.5°).

Discussion

1. Kinetic and Thermodynamic Alkene Binding Selectivities. The diastereomers of *cis*-alkene complexes (*Z*)-**1a–d** (**IV, V**; Scheme II) readily interconvert at room temperature ((*Z*)-**1d**) or below ((*Z*)-**1a–c**). Since syntheses require extended periods between −45 °C and room temperature, it is not possible to measure kinetic alkene binding selectivities. However, the thermodynamic binding selectivities increase as the sizes of the C=C substituents increase. In our earlier studies of analogous *cis*-cycloalkene complexes (**VIII**, Chart I),[4] all NMR data were acquired at room temperature. Thus, we recorded ^{31}P NMR spectra in $CDCl_3$ at low temperatures. In all cases, two resonances were observed at −70 °C. Ratios ranged from 95:5 for cyclopentene (8.98/10.92 ppm) to 85:15 for cyclooctene (9.74/10.67 ppm), with coalescence temperatures near −50 °C. Hence, this class of complexes exhibits similar diastereomeric equilibria.

Importantly, alkyl-substituted *cis*-alkene complexes of **I** give lower equilibrium ratios of diastereomers than the corresponding monosubstituted alkene complexes. Thus, the **IVa/Va** ratio for *cis*-2-butene complex (*Z*)-**1a** (70–84:30–16, −60 to −100 °C; Scheme II) is less than the **IIa/IIIa** ratio for the analogous propene complex (96:4, 95–100 °C; Scheme I).[3b] The *cis*-3-hexene complex (*Z*)-**1b** and the related 1-pentene complex show a similar trend (85:15 vs 97:3). Hence, differences in the free energies of diastereomeric alkyl-substituted *cis* alkene complexes are smaller than those of the corresponding diastereomeric monosubstituted alkene complexes.

This indicates that the addition of a *cis* C=C alkyl substituent to **II** is slightly destabilizing relative to the addition of a *cis* C=C alkyl substituent to **III**. In other words, on the C=C terminus *syn* to the PPh_3 ligand, an alkyl substituent *anti* to the cyclopentadienyl ligand ("down" in **IV**) is slightly destabilizing relative to a substituent *syn* to the cyclopentadienyl ligand ("up" in **V**). This follows from the congested nature of the interstice between the PPh_3 and nitrosyl ligands.[10] However, the

(25) Ittel, S. D.; Ibers, J. A. *Adv. Organomet. Chem.* **1976**, *14*, 33.

Table II. Summary of Crystallographic Data for the *cis* and *trans*-2-Butene Complexes (*Z*)-1a·(CH_2Cl_2) and (*E*)-1a·$(C_5H_{12})_{0.5}$ (*RSS,SRR* Diastereomer)

compound	(*Z*)-**1a**·(CH_2Cl_2)	(*E*)-**1a**·$(C_5H_{12})_{0.5}$
molecular formula	$C_{28}H_{30}BCl_2F_4NOPRe$	$C_{29.5}H_{34}BF_5NOPRe$
formula weight	771.44	722.59
crystal system	monoclinic	monoclinic
space group	$P2_1/n$	$C2/c$
cell dimensions		
a, Å	12.030(1)	28.703(8)
b, Å	22.430(1)	14.454(3)
c, Å	11.385(1)	14.510(4)
β, deg	101.06(1)	109.64(2)
V, Å^3	3014.99	5669.94
Z	4	8
d_{calcd}, g/cm^3 (15 °C)	1.699	1.693
d_{obs}, g/cm^3 (22 °C)	1.706	1.685
crystal dimensions, mm	0.35 × 0.25 × 0.15	0.23 × 0.20 × 0.17
diffractometer	Syntex P$\bar{1}$	Enraf-Nonius CAD-4
radiation, Å	λ(Mo Kα) = 0.710 73	λ(Mo Kα) = 0.709 30
data collection method	θ–2θ	θ–2θ
scan speed, deg/min	2.0	variable (1.0–8.0)
range/indices (hkl)	0–14, 0–26, –13 to +13	0–32, 0–16, –15 to +15
scan range	Kα_1 –1.3 to Kα_2 +1.6	0.80 + 0.34 tan θ
no. of reflections between stds	98	1 X-ray h
total no. of unique data	5852	4759
no. of observed data, $I > 3\sigma(I)$	5559	2820
abs coeff (μ), cm^{-1}	43.62	44.48
% minimum transmission	67.30	71.87
% maximum transmission	99.00	99.80
no. of variables	353	353
$R = \Sigma(\|\|F_o\| - \|F_c\|\|)/\Sigma\|F_o\|$	0.0408	0.0360
$R_w = \Sigma(\|\|F_o\| - \|F_c\|\|)w^{1/2}/\Sigma\|F_o\|w^{1/2}$	0.0438	0.0393
goodness of fit	3.1606	0.5873
Δ/σ (max)	0.002	0.002
$\Delta\rho$ (max), e/Å^3	1.589 (~0.925 Å from Re)	0.785

cis-stilbene complex (*Z*)-**1c** gives a **IVc/Vc** equilibrium ratio (93:7) similar to the **IIc/IIIc** ratio of the corresponding styrene complex (90:10).

The diastereomers of *trans*-alkene complexes (*E*)-**1a–c** (**VI, VII**; Scheme III) interconvert with much higher barriers. Thus, syntheses conducted at lower temperatures give nonequilibrium diastereomer ratios. Possible origins of the lower kinetic selectivities have been discussed earlier.[3c] The greatest difference is observed with *trans*-3-hexene complex (*E*)-**1b**, for which a 52:48 **VIb/VIIb** mixture is obtained after 25% conversion at 60 °C. The much faster reaction of **2** and *trans*-stilbene suggests that a phenyl ring may be the kinetic binding site.

For all three *trans* alkene complexes, the **VI/VII** equilibrium ratios (99:1, >99:1, 98:2; Scheme III) are higher than the **II/III** equilibrium ratios of the corresponding monosubstituted alkene complexes (96:4, 97:3, 90:10, Scheme I).[3c] Thus, diastereomeric *trans*-alkene complexes exhibit greater free energy differences. This trend is complementary to that of *cis*-alkene complexes (*Z*)-**1a,b**, and shows that on the C=C terminus *syn* to the PPh_3 ligand the substituent position in **VII** is destabilizing relative to that in **VI**. Thus, relative to monosubstituted alkenes, *trans*-alkenes give slightly enhanced thermodynamic binding selectivities, and *cis*-alkenes generally give slightly diminished thermodynamic binding selectivities.

To our knowledge, **I** is the only chiral receptor found to date that is capable of binding one enantioface of symmetrical *trans*-alkenes with high thermodynamic selectivities. Other chiral metal fragments for which diastereomeric *trans*-2-butene complexes have been reported are illustrated in Chart III.[2d,26] As explicitly demonstrated with the corresponding monosubstituted alkene complexes,[3] all of the compounds described herein should be readily available in enantiomerically pure form. Thus, there are numerous possibilities for enantioselective syntheses of organic molecules.[27]

2. Isomerization of Alkene Complexes. As shown in Table I, the barriers for isomerization of the less stable *RRS,SSR* diastereomers of *cis*-alkene complexes (*Z*)-**1a–c** to the more stable *RSR,SRS* diastereomers increase as the size of the =CHR substituent increases (R = CH_3, C_2H_5, C_6H_5: 11.0–11.1, 12.6–12.8, 13.2 kcal/mol). The 2D NMR experiments with *cis*-2-butene complex (*Z*)-**1a**, and the spin saturation data for *cis*-1,2-dichloroethylene complex (*Z*)-**1d**, show that isomerization occurs by a simple 180° rotation about the Re–(C=C) bond axis.[21] In all cases, π back-bonding should diminish along the reaction coordinate. Thus, the higher barrier of the *cis*-1,2-dichloroethylene ligand (>17.5 kcal/mol) can be attributed to its superior π acidity, which stabilizes the ground state more than the transition state.

Rotation about the Re–(C=C) axis of *trans*-alkene complexes (*E*)-**1** is, in contrast to *cis*-alkene complexes (*Z*)-**1**, a degenerate process. These barriers also exhibit several interesting trends (Table I). For example, that of the *RSS,SRR* diastereomer of *trans*-2-butene complex (*E*)-**1a** (18.6 kcal/mol) is much higher than that of *cis*-2-butene complex (*Z*)-**1a** (11.0–11.8 kcal/mol). We propose the following explanation. The interconversion of *Z* isomers **IV** and **V** in Scheme II can be accomplished by sequential passage of the =CHR substituents over the medium-sized cyclopentadienyl ligand. No transit over the bulky PPh_3 ligand is required. However, the interconversion of

(26) (a) Boucher, H.; Bosnich, B. *J. Am. Chem. Soc.* **1977**, *99*, 6253. (b) Shinoda, S.; Yamaguchi, Y.; Saito, Y. *Inorg. Chem.* **1979**, *18*, 673.

(27) For additions of alkyl copper nucleophiles, see Peng, T.-S.; Gladysz, J. A. *Tetrahedron Lett.* **1990**, *31*, 4417.

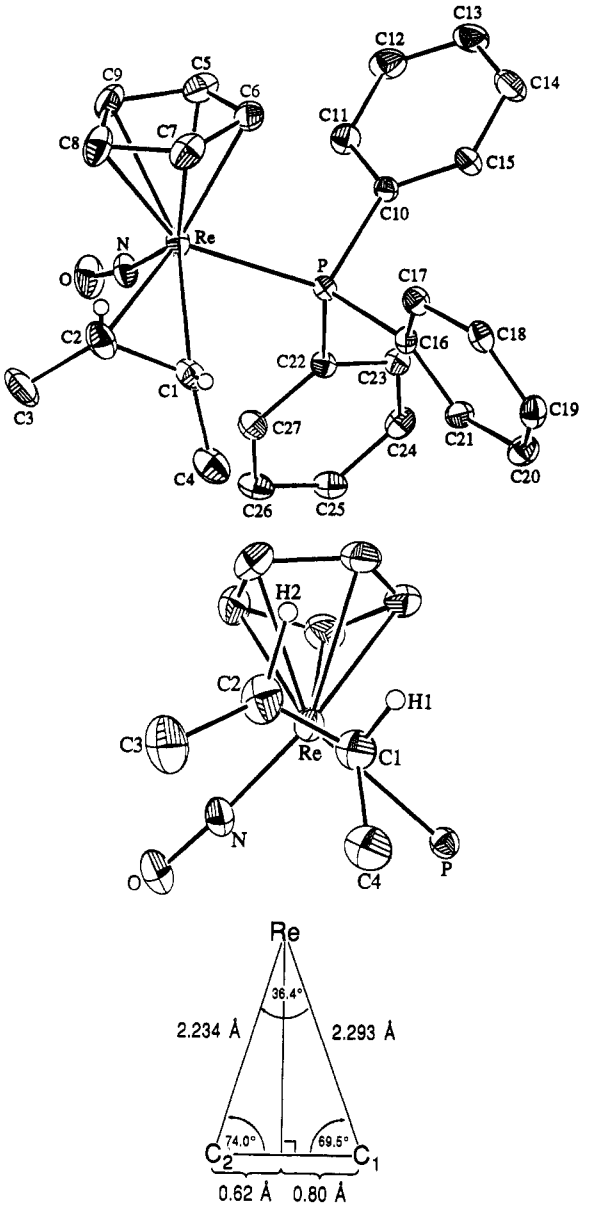

Figure 3. Structure of the cation of *cis*-2-butene complex (*RSR,SRS*)-[(η^5-C_5H_5)Re(NO)(PPh_3)($H_3CHC{=}CH$-CH_3)]$^+BF_4^-$ ((*RSR,SRS*)-**1a**): top, numbering diagram; middle, Newman-type projection with phenyl rings omitted; bottom, view of Re–C$_{1,2}$C plane.

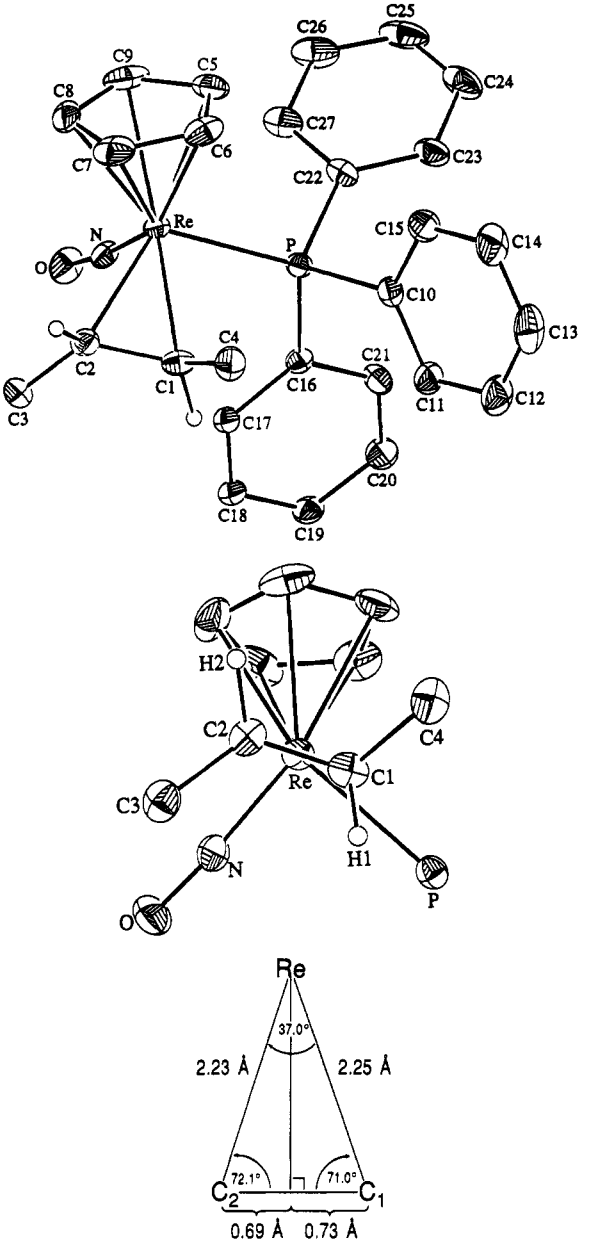

Figure 4. Structure of the cation of *trans*-2-butene complex (*RSS,SRR*)-[(η^5-C_5H_5)Re(NO)(PPh_3)($H_3CHC{=}CH$-CH_3)]$^+BF_4^-$ ((*RSS,SRR*)-**1a**): top, numbering diagram; middle, Newman-type projection with phenyl rings omitted; bottom, view of Re–C$_{1,2}$C plane.

degenerate rotamers of *trans* complexes (Scheme V) requires, at some stage, the passage of a =CHR substituent over the bulky PPh_3 ligand. Thus, barriers are generally higher.

This comparison holds for stilbene complexes (*Z*)-**1c** and the *RSS,SRR* diastereomer of (*E*)-**1c** (12.8–13.5 vs >17.6 kcal/mol). However, the rotational barrier of the less stable *RRR,SSS* diastereomer of (*E*)-**1c** (11.6 kcal/mol) is lower than either of these compounds. Since substituents are forced into the *least* favorable position on each C=C terminus in *RRR,SSS*, diastereomers, we suggest that the low barrier is primarily due to ground-state strain. The transition states for the two (*E*)-**1c** diastereomers would likely involve comparable repulsive interactions between eclipsing =CH phenyl groups and PPh_3 ligands, with the configuration at the opposite =CH terminus of secondary energetic importance. Ground-state strain (and/or π acidity effects) may also contribute to the lower rotational barriers of (*Z*)-**1a–c** compared to the corresponding ethylene complex (16.4 kcal/mol).[3a]

We presently have no information on the mechanism by which the *RRR,SSS* diastereomers of (*E*)-**1a–c** isomerize to *RSS,SRR* diastereomers. With analogous monosubstituted alkene complexes (**II, III**) this process is nondissociative, and based upon an extensive series of experiments an intermediate C-H "σ bond" complex has been proposed.[3c] The isomerization of *trans*-stilbene complex (*E*)-**1c** is much faster than those of monosubstituted alkene complexes, and a mechanistic study is planned.

3. Other Spectroscopic and Structural Properties. The NMR data presented above establish a number of useful correlations that will be important in studies of complexes of **I** and other classes of alkenes.[5,6] For example, with all of the diastereomers **IV–VII** in Scheme I (a) the

Table III. Atomic Coordinates for (*Z*)-1a·(CH_2Cl_2) and (*E*)-1a·(C_5H_{12})$_{0.5}$

	(*Z*)-1a·(CH_2Cl_2)			(*E*)-1a·(C_5H_{12})$_{0.5}$		
atom	*x*	*y*	*z*	*x*	*y*	*z*
Re	0.70905(3)	0.78131(2)	0.94111(3)	0.13053(1)	0.11061(3)	0.49826(3)
P	0.8224(2)	0.8712(1)	0.9778(2)	0.10518(9)	0.2474(2)	0.5654(2)
F1	0.5029(6)	0.1635(4)	0.4763(7)	0.2280(3)	−0.1717(7)	0.7649(6)
F2	0.3287(7)	0.1354(5)	0.4750(7)	0.2175(4)	−0.2944(7)	0.6756(9)
F3	0.4381(8)	0.1556(5)	0.6429(7)	0.1637(4)	−0.1906(8)	0.6327(7)
F4	0.4666(8)	0.0780(4)	0.5453(8)	0.1686(4)	−0.268(1)	0.7556(8)
O	0.8110(8)	0.7317(4)	1.1734(6)	0.0653(3)	0.1635(7)	0.3023(5)
N	0.7648(7)	0.7549(4)	1.0839(7)	0.0895(3)	0.1425(6)	0.3832(5)
C1	0.5638(8)	0.8450(5)	0.9579(9)	0.0822(4)	0.0414(8)	0.5716(7)
C2	0.5279(8)	0.7849(6)	0.961(1)	0.0862(4)	−0.0168(8)	0.4958(8)
C3	0.497(1)	0.7568(7)	1.067(1)	0.0443(4)	−0.0352(9)	0.4036(9)
C4	0.562(1)	0.8865(7)	1.056(1)	0.1063(5)	0.0133(9)	0.6775(8)
C5	0.816(1)	0.7348(5)	0.8222(9)	0.2099(4)	0.1621(9)	0.557(1)
C6	0.753(1)	0.7780(5)	0.7507(9)	0.2077(4)	0.086(1)	0.6136(8)
C7	0.638(1)	0.7641(5)	0.7401(9)	0.1963(4)	0.009(1)	0.554(1)
C8	0.627(1)	0.7111(5)	0.807(1)	0.1922(4)	0.039(1)	0.460(1)
C9	0.742(1)	0.6930(5)	0.852(1)	0.2012(4)	0.131(1)	0.4642(8)
C10	0.9532(7)	0.8629(4)	0.9207(8)	0.1165(4)	0.2464(8)	0.6964(7)
C11	1.0259(8)	0.8165(5)	0.9659(9)	0.0783(4)	0.2459(9)	0.7350(8)
C12	1.1247(9)	0.8079(6)	0.924(1)	0.0887(5)	0.245(1)	0.8339(9)
C13	1.1520(9)	0.8451(6)	0.838(1)	0.1356(6)	0.245(1)	0.8954(8)
C14	1.080(1)	0.8900(6)	0.793(1)	0.1739(5)	0.243(1)	0.8601(9)
C15	0.9801(8)	0.8992(5)	0.8334(9)	0.1643(4)	0.246(1)	0.7611(9)
C16	0.7631(7)	0.9407(4)	0.9099(8)	0.0401(3)	0.2785(7)	0.5139(7)
C17	0.7052(8)	0.9393(4)	0.7905(8)	0.0043(3)	0.2221(8)	0.4499(7)
C18	0.6640(8)	0.9919(5)	0.7352(8)	−0.0448(4)	0.2492(9)	0.4150(8)
C19	0.6752(8)	1.0455(4)	0.797(1)	−0.0595(4)	0.3303(9)	0.4433(8)
C20	0.7319(9)	1.0469(5)	0.914(1)	−0.0244(4)	0.387(1)	0.5076(9)
C21	0.7763(8)	0.9945(4)	0.9717(8)	0.0244(4)	0.3624(8)	0.5415(8)
C22	0.8771(7)	0.8900(4)	1.1355(7)	0.1366(4)	0.3501(8)	0.5453(8)
C23	0.9771(8)	0.9231(4)	1.1633(8)	0.1510(4)	0.4200(8)	0.612(1)
C24	1.0176(8)	0.9409(5)	1.2817(9)	0.1734(5)	0.4995(9)	0.592(1)
C25	0.9582(9)	0.9253(5)	1.3696(9)	0.1808(5)	0.509(1)	0.506(1)
C26	0.8621(9)	0.8915(5)	1.3436(9)	0.1675(5)	0.442(1)	0.438(1)
C27	0.8219(8)	0.8735(5)	1.2260(8)	0.1447(4)	0.3616(8)	0.456(1)
C28	0.638(1)	0.0391(8)	0.366(1)	0.0533(5)	0.5177(9)	0.2747(9)
C29				0.0266(6)	0.584(1)	0.773(1)
C30				−0.0498(5)	0.532(1)	0.732(1)
B	0.4308(6)	0.1336(3)	0.5347(6)	0.1953(5)	−0.229(1)	0.706(1)
C11	0.7670(3)	0.0561(2)	0.4519(3)			
C12	0.6376(3)	0.0366(2)	0.2157(3)			
H1	0.5000	0.8613	0.8887	0.0488	0.0625	0.5625
H2	0.4707	0.7793	0.8594	0.1074	−0.0820	0.5214

C=C ^{13}C NMR resonance of the carbon *syn* to the PPh_3 ligand is downfield of that *anti* to the PPh_3 ligand, and gives a larger J_{CP}; (b) the ^1H NMR resonance of the =CH group *syn* to the PPh_3 ligand is upfield of that *anti* to the PPh_3 ligand, and (when resolved) gives a larger J_{HP}. The ^1H NMR chemical shifts of the methyl groups in diastereomeric 2-butene, propene, and isobutene complexes of **I** follow the shielding patterns summarized in **X** (Chart II). Many trends other than those explicitly noted above can also be discerned.

As expected from the resonance forms in Scheme I, the C–C bond lengths in crystalline 2-butene complexes (*Z*)-**1a** and (*E*)-**1a** [1.417(9), 1.42(2) Å] are between those of the CH_2–CH_2 bond in *n*-butane [1.531(2) Å],[27] and the C=C bonds in the free alkenes [1.348(1), 1.347(3) Å].[28] In (*Z*)-**1a**, the Re–C1 bond is longer than the Re–C2 bond [2.293(7) vs 2.234(6) Å], and the Re–C1–C2 angle is smaller than the Re–C2–C1 angle [69.5(4)° vs 74.0(4)°]. Thus, the *cis*-2-butene ligand is not bound symmetrically, but is "slipped" slightly toward C2. However, the corresponding bond lengths and angles are identical within experimental error in the *trans* complex (*E*)-**1a**.

Monosubstituted alkene complexes of **I** usually show a small amount of slippage in the opposite direction.[3a,b,5] We speculate that in 1,2-disubstituted alkene complexes of **I**, steric repulsion between the PPh_3 ligand and *syn* =CHR terminus serves to slightly lengthen the corresponding Re–C bond. The crystal structure of the *methyl*cyclopentadienyl cyclopentene complex $[(\eta^5\text{-}C_5H_4CH_3)Re(NO)(PPh_3)\overline{CH{=}CH(CH_2)_3}]^+BF_4^-$ (**4**) has also been determined.[4] It exhibits equal Re–C bond lengths.

The 2-butene ligand conformations in crystalline (*Z*)-**1a** and (*E*)-**1a** deviate from those shown in idealized structures **IV** and **VI**. The angles of the $\overline{Re\text{–}C{=}C}$ planes with the Re–P and Re–N bonds, which are 0° and ±90° in **IV** and **VI**, provide one of several measures. In (*Z*)-**1a**, these angles (12.3°, 69.5°) are comparable to those of cyclopentene complex **4** (8.8°, 73.6°), and monosubstituted alkene complexes of **I** (15–18°, 71–70°).[3a,b,5] In all cases, the deviation is in a counterclockwise torsional direction from the projections in Scheme I. The distortion in (*E*)-**1a** (22.6°, 66.4°) is the largest observed to date. We suggest that this is driven by repulsion between the PPh_3 ligand and the *syn* =CH methyl group (C4). Indeed, when (*Z*)-

(28) Calloman, J. H.; Hirota, E.; Iijima, T.; Kuchitsu, K.; Lafferty, W. J. In *Landolt-Börnstein Numerical Data and Functional Relationship in Science and Technology*; Madelung, O., Ed. in Chief; Spring-Verlag: New York, 1987; Vol. 15; *Structure Data of Free Polyatomic Molecules*; Hellwege, K.-H.; Hellwege, A. M., volume Eds.; p 428, 442, 478.

Table IV. Selected Bond Lengths (Å), Bond Angles (deg), and Torsion Angles (deg) in (*Z*)-1a·(CH_2Cl_2) and (*E*)-1a·(C_5H_{12})$_{0.5}$

	(*Z*)-1a·(CH_2Cl_2)	(*E*)-1a·(C_5H_{12})$_{0.5}$
Re–P	2.426(1)	2.421(4)
Re–N	1.740(5)	1.75(1)
Re–C1	2.293(7)	2.25(1)
Re–C2	2.234(6)	2.23(1)
Re–C5	2.286(7)	2.27(2)
Re–C6	2.329(6)	2.31(1)
Re–C7	2.317(6)	2.31(2)
Re–C8	2.286(7)	2.27(2)
Re–C9	2.291(6)	2.26(2)
P–C10	1.824(5)	1.82(1)
P–C16	1.823(5)	1.82(1)
P–C22	1.839(5)	1.81(2)
O–N	1.184(6)	1.18(1)
C1–C2	1.417(9)	1.42(2)
C1–C4	1.454(9)	1.51(2)
C2–C3	1.471(9)	1.49(2)
C5–C6	1.391(9)	1.39(2)
C5–C9	1.377(9)	1.36(3)
C6–C7	1.406(9)	1.38(3)
C7–C8	1.428(9)	1.40(3)
C8–C9	1.44(1)	1.35(3)
P–Re–N	91.1(2)	88.4(4)
P–Re–C1	83.1(2)	81.7(4)
P–Re–C2	118.7(2)	115.7(4)
N–Re–C1	107.3(2)	104.2(6)
N–Re–C2	97.3(2)	90.3(6)
C1–Re–C2	36.4(2)	37.0(5)
Re–P–C10	110.4(2)	116.2(5)
Re–P–C16	118.5(2)	116.3(5)
Re–P–C22	116.3(2)	111.8(5)
Re–N–O	170.9(5)	174(1)
Re–C1–C2	69.5(4)	71.0(8)
Re–C1–C4	125.8(5)	117(1)
C2–C1–C4	122.8(6)	120(1)
Re–C2–C1	74.0(4)	72.1(8)
Re–C2–C3	118.0(5)	116(1)
C1–C2–C3	123.5(7)	123(1)
C6–C5–C9	108.6(7)	107(2)
C5–C6–C7	108.0(6)	109(2)
C6–C7–C8	109.2(6)	106(2)
C7–C8–C9	104.4(6)	108(2)
C5–C9–C8	109.7(6)	110(2)
C4–C1–C2–C3	–7(2)	–139(1)
C4–C1–C2–H2	136	0
H1–C1–C2–C3	–120	–7
H1–C1–C2–H2	23	131

Chart III. Binding Selectivities of Other Chiral Metal Fragments and *trans*-2-Butene[2d,26]

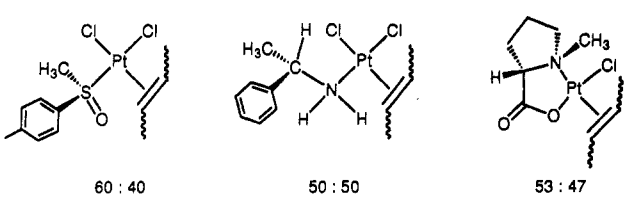

60 : 40 50 : 50 53 : 47

1a and (*E*)-1a are superimposed via their N–Re–P linkages in stereo, the conformational "response" of the PPh_3 ligand to this C4 methyl group is vividly illustrated.

4. Conclusion. This study has provided efficient syntheses of symmetrical *cis*- and *trans*-alkene complexes of the chiral rhenium Lewis acid **I**. Four configurational diastereomers are observed, and their NMR properties have been carefully defined. Rotation about the Re–(C=C) axis interconverts *cis*-alkene complex diastereomers, and makes equivalent the =CHR termini within each *trans*-alkene complex diastereomer. Diastereomeric *trans*-alkene complexes interconvert by a higher energy process, the mechanism of which remains to be probed.

These efforts also lay the needed groundwork for (1) studies of analogous optically active complexes, which may have use in enantioselective organic syntheses, (2) syntheses and structural analyses of adducts of **I** and unsymmetrical *cis*- and *trans*-alkenes, where there is the potential for twice as many configurational diastereomers, and (3) investigations of complexes of **I** and α,β-unsaturated organic carbonyl compounds. The first two are in progress, and the third is described in the following paper.[6]

Experimental Section[29]

(*Z*)-[(η^5-C_5H_5)Re(NO)(PPh_3)(CH_3HC=$CHCH_3$)]$^+BF_4^-$ ((*Z*)-1a). A Schlenk tube with an O-ring-sealed Teflon stopcock was charged with (η^5-C_5H_5)Re(NO)(PPh_3)(CH_3) (**5**, 0.172 g, 0.310 mmol),[30] C_6H_5Cl (9 mL), and a stirbar. The tube was cooled to –45 °C (CH_3CN/CO_2 bath) and HBF_4·OEt_2 (33 μL, 0.31 mmol) was added with stirring. After 0.5 h, excess *cis*-2-butene was added and the stopcock was closed. The cold bath was removed and the solution was stirred for 6 h. The mixture was filtered and solvent was removed *in vacuo*. The residue was dissolved in CH_2Cl_2 (2 mL) and the solution was added dropwise to stirring hexane (80 mL). The resulting tan powder was collected by filtration, washed with pentane (2 × 1 mL), and dried *in vacuo* to give (*Z*)-1a (0.179 g, 0.260 mmol, 84%). Dec pt: 97–98 °C. A CH_2Cl_2 solution of (*Z*)-1a was layered with ether. This gave (*Z*)-1a·(CH_2Cl_2) as red-brown prisms that were used for X-ray analysis. Anal. Calcd for $C_{27}H_{28}BF_4NOPRe·CH_2Cl_2$: C, 43.59; H, 3.92. Found: C, 43.46; H, 3.83. IR (cm^{-1}, thin film): ν_{NO} 1717 vs.

NMR, (*Z*)-1a:[31] ^1H (δ) 7.78–7.26 (m, PPh_3), 5.70 (s, C_5H_5), 4.29 (m, =CH *anti* to PPh_3), 3.51 (m, =CH *syn* to PPh_3), 1.89 (d, J_{HH} = 5.1, CH_3 *anti* to PPh_3), 1.70 (d, J_{HH} = 5.1, CH_3 *syn* to PPh_3); $^{13}C\{^1H\}$ (ppm) 133.4 (d, J_{CP} = 9.8, *o*-Ph), 132.0 (s, *p*-Ph), 130.3 (d, J_{CP} = 56.3, *i*-Ph), 129.4 (d, J_{CP} = 10.7, *m*-Ph), 97.6 (s, C_5H_5), 53.4 (d, J_{CP} = 3.3, =C *syn* to PPh_3), 50.4 (s, =C *anti* to PPh_3), 18.3 (s, CH_3 *anti* to PPh_3), 16.2 (s, CH_3 *syn* to PPh_3); $^{31}P\{^1H\}$ (ppm) 8.0 (s).

NMR (CD_2Cl_2, –100 °C), *RSR,SRS* diastereomer: ^1H (δ, referenced to $CHDCl_2$) 7.76–6.88 (m, PPh_3), 5.62 (s, C_5H_5), 4.18 (m, =CH *anti* to PPh_3), 2.86 (m, =CH *syn* to PPh_3), 2.04 (d, J_{HH} = 5.1, CH_3 *anti* to PPh_3), 1.58 (d, J_{HH} = 5.0, CH_3 *syn* to PPh_3); $^{31}P\{^1H\}$ (ppm, referenced to H_3PO_4 at 25 °C) 8.2 (s). *RRS,SSR* diastereomer: ^1H (δ) 5.64 (s, C_5H_5), 3.91 (m, =CH *anti* to PPh_3),[32] 3.79 (m, =CH *syn* to PPh_3),[32] 2.28 (d, J_{HH} = 4.9, CH_3 *anti* to PPh_3), 0.65 (d, J_{HH} = 4.9, CH_3 *syn* to PPh_3); $^{31}P\{^1H\}$ (ppm) 10.8 (s).

(*Z*)-[(η^5-C_5H_5)Re(NO)(PPh_3)(C_2H_5HC=CHC_2H_5)]$^+BF_4^-$ ((*Z*)-1b). Complex **5** (0.129 g, 0.230 mmol), C_6H_5Cl (4 mL), HBF_4·OEt_2 (26 μL, 0.24 mmol), and *cis*-3-hexene (85 μL, 0.69 mmol) were combined in a procedure analogous to that given for (*Z*)-1a. After 5 h, an identical workup gave (*Z*)-1b (0.156 g, 0.220 mmol, 95%) as a tan powder. Mp: 174–176 °C dec. Anal. Calcd for $C_{29}H_{32}BF_4NOPRe$: C, 48.75; H, 4.51. Found: C, 48.71; H, 4.49. IR (cm^{-1}, thin film): ν_{NO} 1716 vs.

NMR, (*Z*)-1b:[31] ^1H (δ, 56 °C) 7.56–7.31 (m, PPh_3), 5.73 (s, C_5H_5), 4.36 (m, =CH *anti* to PPh_3), 2.97 (m, =CH *syn* to PPh_3), 2.18 (m, CH_2), 1.79 (m, CH_2'), 1.11 (t, J_{HH} = 7.0, CH_3), 0.81 (t, J_{HH} = 7.0, CH_3'); $^{13}C\{^1H\}$ (ppm) 133.5 (d, J_{CP} = 9.7, *o*-Ph), 132.0

(29) General procedures were identical with those described in a previous paper.[3b] The *cis*-3-hexene (TCI: Tokyo Kasei) and other alkenes (Aldrich) were used as received.

(30) Agbossou, F.; O'Connor, E. J.; Garner, C. M.; Quirós Méndez, N.; Fernández, J. M.; Patton, A. T.; Ramsden, J. A.; Gladysz, J. A. *Inorg. Syn.* **1992**, *29*, 211.

(31) NMR spectra were recorded in $CDCl_3$ at ambient probe temperature and referenced to $Si(CH_3)_4$ (^1H, δ 0.00), $CDCl_3$ (^{13}C, 77.0 ppm), or external 85% H_3PO_4 (^{31}P, 0.00 ppm) unless noted. All coupling constants (J) are in Hz.

(32) Assigned by analogy to the chemical shift trend rigorously established for the *RRS,SSR* diastereomer of (*Z*)-1d.

(s, *p*-Ph), 130.2 (s, part of *i*-Ph),[33] 129.4 (d, J_{CP} = 11.3, *m*-Ph), 97.5 (s, C_5H_5), 58.4 (br s, =C *syn* to PPh_3), 55.7 (s, =C *anti* to PPh_3), 25.7 (s, CH_2), 25.1 (s, CH_2'), 19.2 (s, CH_3), 17.0 (s, CH_3'); $^{31}P\{^1H\}$ (ppm) 9.9 (s).

^1H NMR (δ, −62 °C), *RSR,SRS* diastereomer: 7.70–7.11 (m, PPh_3), 5.77 (s, C_5H_5), 4.38 (m, =CH *anti* to PPh_3),[34] 2.67 (m, =CH *syn* to PPh_3),[34] 2.47, 2.03 (2m, =CHCH_2 *anti* to PPh_3),[34] 1.76 (m, =CHCH_2 *syn* to PPh_3),[34] 1.24 (t, J_{HH} = 6.7, CH_3 *anti* to PPh_3),[34] 0.60 (t, J_{HH} = 6.7, CH_3 *syn* to PPh_3).[34] *RRS,SSR* diastereomer (partial): 5.73 (s, C_5H_5), 3.86 (m, =CH *anti* to PPh_3),[32] 3.48 (m, =CH *syn* to PPh_3),[32] 1.35 (t, J_{HH} = 6.6, CH_3 *anti* to PPh_3),[35] 0.88 (t, J_{HH} = 6.8, CH_3 *syn* to PPh_3).[35]

(*Z*)-$[(\eta^5\text{-}C_5H_5)Re(NO)(PPh_3)(C_6H_5HC{=}CHC_6H_5)]^+BF_4^-$ ((*Z*)-1c). Complex **5** (0.112 g, 0.200 mmol), C_6H_5Cl (2 mL), $HBF_4{\cdot}OEt_2$ (24 μL, 0.22 mmol), and *cis*-stilbene (178 μL, 1.00 mmol) were combined in a procedure analogous to that given for (*Z*)-**1a**. After 16 h, a similar workup gave (*Z*)-**1c** (0.109 g, 0.135 mmol, 67%) as a light tan powder. Mp: 138–141 °C dec. Anal. Calcd for $C_{37}H_{32}BF_4NOPRe$: C, 54.82; H, 3.98. Found: C, 54.02; H, 3.90. IR (cm^{-1}, thin film): ν_{NO} 1722 vs. MS:[36] 724 (M^+, 15%), 544 ($M^+ - C_{14}H_{12}$, 100%).

^1H NMR, (*Z*)-**1c** (δ, 70 °C):[31] 7.70–6.42 (m, PPh_3, 2CPh), 5.88 (s, C_5H_5), 5.28 (d, J_{HH} = 11.0, =CH *anti* to PPh_3), 4.73 (dd, J_{HH} = 11.0, J_{HP} = 8.7, =CH *syn* to PPh_3).

NMR (−30 °C), *RSR,SRS* diastereomer:[31] ^1H (δ) 7.56–6.65 (m, PPh_3 and 8H of 2CPh), 5.98 (s, C_5H_5), 5.85 (d, J_{HH} = 7.1, 2H of 2CPh), 5.35 (d, J_{HH} = 11.6, =CH *anti* to PPh_3), 4.48 (dd, J_{HH} = 11.6, J_{HP} = 11.6, =CH *syn* to PPh_3); $^{13}C\{^1H\}$ (ppm) 133.6 (d, J_{CP} = 9.3, *o*-PPh), 131.9 (s, *p*-PPh), 129.1 (d, J_{CP} = 52.2, *i*-PPh), 129.0 (d, J_{CP} = 10.7, *m*-PPh), 139.8, 137.2, 131.8, 130.2, 128.5, 127.1, 127.1, 126.9 (8 s, 2C*Ph*), 98.4 (s, C_5H_5), 59.0 (br s, =C *syn* to PPh_3), 52.4 (s, =C *anti* to PPh_3); $^{31}P\{^1H\}$ (ppm) 3.7 (s). *RRS,SSR* diastereomer (partial): ^1H (δ) 5.55 (s, C_5H_5); $^{13}C\{^1H\}$ (ppm) 101.1 (s, C_5H_5); $^{31}P\{^1H\}$ (ppm) 5.8 (s).

(*Z*)-$[(\eta^5\text{-}C_5H_5)Re(NO)(PPh_3)(ClHC{=}CHCl)]^+BF_4^-$ ((*Z*)-1d). Complex **5** (0.169 g, 0.300 mmol), C_6H_5Cl (3 mL), $HBF_4{\cdot}OEt_2$ (33 μL, 0.30 mmol), and *cis*-1,2-dichloroethylene (200 μL, 2.60 mmol) were combined in a procedure analogous to that given for (*Z*)-**1a**. After 24 h, the resulting ivory powder was collected by filtration (0.148 g). Solvent was removed from the filtrate *in vacuo*, and the residue was reprecipitated from CH_2Cl_2/ether as with (*Z*)-**1a** to give a second crop of product (0.032 g). The crops were combined, washed with pentane, and dried *in vacuo* to give (*Z*)-**1d** (0.180 g, 0.248 mmol, 83%) as a 59:41[14] mixture of *RSR,SRS*/*RRS,SSR* diastereomers. Mp: 106–107 °C dec. Anal. Calcd for $C_{25}H_{22}BCl_2F_4NOPRe$: C, 41.28; H, 3.05; Cl, 9.75. Found: C, 41.24; H, 3.09; Cl, 9.82. IR (cm^{-1}, thin film): ν_{NO} 1755 vs.

NMR, *RSR,SRS* diastereomer:[31] ^1H (δ) 7.64–7.42 (m, PPh_3), 5.93 (s, C_5H_5), 5.50 (dd, J_{HH} = 5.5, J_{HP} = 1.5, =CH *anti* to PPh_3), 4.68 (dd, J_{HH} = 5.5, J_{HP} = 13.7, =CH *syn* to PPh_3); $^{13}C\{^1H\}$ (ppm) 133.8 (d, J_{CP} = 10.1, *o*-Ph), 132.8 (d, J_{CP} = 2.6, *p*-Ph), 130.0 (d, J_{CP} = 11.3, *m*-Ph), 127.7 (d, J_{CP} = 48.1, *i*-Ph), 104.0 (s, C_5H_5), 56.0 (d, J_{CP} = 7.9, =C *syn* to PPh_3), 54.9 (s, =C *anti* to PPh_3); $^{31}P\{^1H\}$ (ppm) 6.4 (s). *RRS,SSR* diastereomer (partial): ^1H (δ) 6.10 (dd, J_{HH} = 6.4, J_{HP} = 2.1, =CH, *anti* to PPh_3), 5.90 (s, C_5H_5), 5.04 (dd, J_{HH} = 6.4, J_{HP} = 9.0, =CH *syn* to PPh_3); $^{13}C\{^1H\}$ (ppm) 133.3 (d, J_{CP} = 10.1, *o*-Ph), 132.4 (d, J_{CP} = 2.6, *p*-Ph), 129.5 (d, J_{CP} = 11.3, *m*-Ph), 128.5 (d, J_{CP} = 47.3, *i*-Ph), 99.4 (s, C_5H_5), 58.3 (d, J_{CP} = 8.8, =C *syn* to PPh_3), 49.6 (s, =C *anti* to PPh_3); $^{31}P\{^1H\}$ (ppm) 6.9 (s).

(*E*)-$[(\eta^5\text{-}C_5H_5)Re(NO)(PPh_3)(CH_3HC{=}CHCH_3)]^+BF_4^-$ ((*E*)-1a). A. Complex **5** (0.169 g, 0.303 mmol), C_6H_5Cl (9 mL), $HBF_4{\cdot}OEt_2$ (33 μL, 0.30 mmol), and excess *trans*-2-butene were combined in a procedure analogous to that given for (*Z*)-**1a**. After 6 days, an identical workup gave pale yellow (*E*)-**1a** (0.179 g, 0.260 mmol, 87%) as a 77:10:13 mixture of *RSS,SRR*/*RRR,SSS* diastereomers and contaminating (*Z*)-**1a**. **B.** Complex **5** (0.112 g, 0.200 mmol), C_6H_5Cl (8 mL), $HBF_4{\cdot}OEt_2$ (24 μL, 0.22 mmol), and excess *trans*-2-butene were analogously combined. The cold bath was removed. After 1 h, the tube was transferred to a 95 °C bath and stirred for 20 h. A ^{31}P NMR spectrum of an aliquot showed no trace of (*Z*)-**1a**. The mixture was filtered into hexane (80 mL). The resulting tan powder was collected by filtration, washed with pentane, and dried under oil pump vacuum to give (*E*)-**1a** (0.126 g, 0.184 mmol, 92%) as a 99:1 mixture of the *RSS,SRR*/*RRR,SSS* diastereomers. Dec pt: 164–168 °C. Anal. Calcd for $C_{27}H_{28}BF_4NOPRe$: C, 47.24; H, 4.11. Found: C, 47.05; H, 4.12. A CH_2Cl_2 solution of this sample was layered with pentane. This gave yellow prisms of (*E*)-**1a**·$(C_5H_{12})_{0.5}$ that were used for X-ray analysis. IR (cm^{-1}, thin film): ν_{NO} 1720 vs.

NMR, *RSS,SRR* diastereomer:[31] ^1H (δ) 7.59–7.27 (m, PPh_3), 5.85 (s, C_5H_5), 4.50 (ddq, J_{HH} = 12.5, 6.1, J_{HP} = 1.7, =CH *anti* to PPh_3), 3.08 (ddq, J_{HH} = 12.5, 6.1, J_{HP} = 5.4, =CH *syn* to PPh_3), 2.09 (d, J_{HH} = 6.1, CH_3 *anti* to PPh_3), 1.35 (d, J_{HH} = 6.1, CH_3 *syn* to PPh_3); $^{13}C\{^1H\}$ (ppm) 133.3 (d, J_{CP} = 10.0, *o*-Ph), 132.0 (d, J_{CP} = 2.5, *p*-Ph), 129.6 (d, J_{CP} = 10.9, *m*-Ph),[33] 97.2 (s, C_5H_5), 56.2 (d, J_{CP} = 5.3, =C *syn* to PPh_3), 50.2 (s, =C *anti* to PPh_3), 23.9 (s, CH_3 *anti* to PPh_3), 22.4 (s, CH_3 *syn* to PPh_3); $^{31}P\{^1H\}$ (ppm) 7.7 (s). *RRR,SSS* diastereomer (partial): ^1H (δ) 5.68 (s, C_5H_5), 2.18 (d, J_{HH} = 5.1, CH_3 *anti* to PPh_3), 1.82 (d, J_{HH} = 5.1, CH_3 *syn* to PPh_3); $^{31}P\{^1H\}$ (ppm) 7.1 (s).

(*E*)-$[(\eta^5\text{-}C_5H_5)Re(NO)(PPh_3)(C_2H_5HC{=}CHC_2H_5)]^+BF_4^-$ ((*E*)-1b). A. Complex **5** (0.059 g, 0.100 mmol), C_6H_5Cl (1 mL), $HBF_4{\cdot}OEt_2$ (11 μL, 0.10 mmol), and *trans*-3-hexene (63 μL, 0.50 mmol) were combined in a 5-mm NMR tube in a procedure similar to that given for (*Z*)-**1a**. The tube was transferred to a NMR probe, which was gradually warmed. At 60 °C, a ^{31}P NMR spectrum showed that (*E*)-**1b** had formed as a 52:48 mixture of *RSS,SRR*/*RRR,SSS* diasteromers (7.5, 7.0 ppm; ca. 25% conversion). The sample was chromatographed on a 10 × 0.6 cm silica column using acetone/CH_2Cl_2 (5:95, v/v). This gave (*E*)-**1b** (0.014 g, 0.020 mmol, 20%) as a 60:40 *RSS,SRR*/*RRR,SSS* mixture (with minor impurities), which was used for NMR characterization of the minor diastereomer. **B.** Complex **5** (0.112 g, 0.201 mmol), C_6H_5Cl (4 mL), $HBF_4{\cdot}OEt_2$ (22 μL, 0.20 mmol), and *trans*-3-hexene (125 μL, 1.01 mmol) were combined in a Schlenk tube in a procedure analogous to that given for (*Z*)-**1a**. The mixture was stirred at room temperature for 3.5 h and then 85 °C for 18 h. A ^{31}P NMR spectrum showed no trace of the *RRR,SSS* diastereomer of (*E*)-**1b**. A workup similar to that used for (*Z*)-**1a** gave (*E*)-**1b** (0.123 g, 0.172 mmol, 86%) as a tan powder, >99:<1 *RSS,SRR*/*RRR,SSS*. Dec pt: 164–168 °C. Anal. Calcd for $C_{29}H_{32}BF_4NOPRe$: C, 48.75; H, 4.51. Found: C, 48.56; H, 4.46. IR (cm^{-1}, thin film): ν_{NO} 1721 vs.

NMR, *RSS,SRR* diastereomer:[31] ^1H (δ) 7.59–7.27 (m, PPh_3), 5.85 (s, C_5H_5), 4.25 (m, =CH *anti* to PPh_3), 2.83 (m, =CH *syn* to PPh_3), 2.05 (dq, J_{HH} = 7.0, 7.0, CH_2), 1.93 (dq, J_{HH} = 7.0, 7.0, CH_2'), 1.17 (t, J_{HH} = 7.0, CH_3), 0.81 (t, J_{HH} = 7.0, CH_3'); $^{13}C\{^1H\}$ (ppm) 133.2 (d, J_{CP} = 10.2, *o*-Ph), 132.1 (s, *p*-Ph), 129.5 (d, J_{CP} = 10.7, *m*-Ph),[33] 97.0 (s, C_5H_5), 61.8 (br s, =C *syn* to PPh_3), 56.3 (s, =C *anti* to PPh_3), 32.5 (s, CH_2), 31.5 (s, CH_2'), 20.9 (s, CH_3), 17.9 (s, CH_3'): $^{31}P\{^1H\}$ (ppm) 7.5 (s). *RRR,SSS* diastereomer (partial): ^1H (δ) 5.81 (s, C_5H_5), 1.19 (t, J_{HH} = 6.9, CH_3), 1.12 (t, J_{HH} = 6.8, CH_3'); $^{31}P\{^1H\}$ (ppm) 7.1 (s).

(*E*)-$[(\eta^5\text{-}C_5H_5)Re(NO)(PPh_3)(C_6H_5HC{=}CHC_6H_5)]^+BF_4^-$ ((*E*)-1c). A. Complex **5** (0.112 g, 0.200 mmol), C_6H_5Cl (2 mL), $HBF_4{\cdot}OEt_2$ (24 μL, 0.22 mmol), and *trans*-stilbene (180 μL, 1.00 mmol) were combined in a procedure analogous to preparation B of (*E*)-**1a**. After 16 h, a similar workup gave light tan (*E*)-**1c** (0.085 g, 0.105 mmol, 53%) as a 76:24 mixture of *RSS,SRR*/*RRR,SSS* diastereomers. **B.** The preceding product was chromatographed on a 15 × 1.3 cm silica column using acetone/CH_2Cl_2 (2.5:97.5, v/v). Fractions were combined and solvents removed *in vacuo* to give two light yellow samples: (1) a 11:89 *RSS,SRR*/*RRR,SSS* mixture (0.019 g, 0.023 mmol) [IR (cm^{-1}, thin film): ν_{NO} 1732 vs] and (2) a 97:3 *RSS,SRR*/*RRR,SSS* mixture (0.046

(33) *Ipso* carbon was not located, or one line of doublet was obscured.
(34) This assignment was confirmed by a decoupling experiment (supplementary material).
(35) This assignment is made from the pattern of methyl group coalescence with the *RSR,SRS* diastereomer (text and Table I).
(36) (+)-FAB, 5 kV, Ar, 3-nitrobenzyl alcohol/$CHCl_3$ matrix, *m/z* (relative intensity), ^{187}Re.

g, 0.057 mmol) [Mp: 151–153 °C dec (intermediate fractions gave samples of intermediate composition)]. Crystallization of the latter from layered CH_2Cl_2/hexane gave brown-yellow needles. Mp: 162–164 °C dec. Anal. Calcd for $C_{37}H_{32}BF_4NOPRe$: C, 54.82; H, 3.98; N, 1.73. Found: C, 54.11; H, 3.99; N, 1.71. IR (cm^{-1}, thin film): ν_{NO} 1732 vs. MS:[36] 724 (M^+, 17%), 544 (M^+-$C_{14}H_{12}$, 100%). **C.** A 5-mm NMR tube was charged with $CDCl_3$ (0.5 mL) and the first sample from the previous experiment. After 48 h at room temperature, a ^1H NMR spectrum showed a 56:44 *RSS,SRR/RRR,SSS* ratio. The probe was warmed to 95 °C. After 10 min, the *RSS,SRR/RRR,SSS* ratio was 90:10. **D.** Complex **5** (0.112 g, 0.200 mmol), C_6H_5Cl (2 mL), HBF_4·OEt_2 (24 μL, 0.22 mmol), and *trans*-stilbene (180 μL, 1.00 mmol) were combined in a procedure analogous to A. The sample was stirred for 12 h at 95 °C. A similar workup gave (*E*)-**1c** (0.159 g, 0.196 mmol, 98%) as a 98:2 *RSS,SRR/RRR,SSS* mixture.

NMR, *RSS,SRR* diastereomer:[31] ^1H (δ) 7.80–7.00 (m, PPh_3 and 8H of 2CPh), 6.27 (d, J_{HH} = 7.2, 2H of CPh), 6.26 (d, J_{HH} = 12.4, =CH *anti* to PPh_3), 5.82 (s, C_5H_5), 4.48 (dd, J_{HH} = 12.4, J_{HP} = 7.6, =CH *syn* to PPh_3); $^{13}C\{^1H\}$ (ppm) 133.2 (br s, *o*-PPh), 132.2 (s, *p*-PPh), 129.5 (br s, *m*-PPh),[33] 141.2, 140.4, 128.8, 128.4, 127.5, 127.2, 126.9, 126.2 (8 s, 2C*Ph*), 99.1 (s, C_5H_5), 57.1 (d, J_{CP} = 3.1, =C *syn* to PPh_3), 50.4 (s, =C *anti* to PPh_3); $^{31}P\{^1H\}$ (ppm) 5.4 (s). *RRR,SSS* diastereomer: ^1H (δ) 7.80–6.75 (m, PPh_3 and 2CPh), 5.38 (s, C_5H_5), 4.81 (br s, 2 =CH); $^{13}C\{^1H\}$ (ppm) 133.7 (d, J_{CP} = 10.0, *o*-PPh), 131.8 (s, *p*-PPh), 129.1 (d, J_{CP} = 10.7, *m*-PPh),[33] 141.3, 128.8, 127.8, 126.2 (4 s, 2C*Ph*), 101.4 (s, C_5H_5), 53.0 (br s, 2 =C); $^{31}P\{^1H\}$ (ppm) 4.0 (s). *RRR,SSS* diastereomer (−70 °C): ^1H (δ) 8.05–6.75 (m, PPh_3 and 9H of 2CPh), 5.91 (d, J_{HH} = 7.0, 1H of CPh), 5.44 (s, C_5H_5), 5.38 (d, J_{HH} = 12.7, =CH *anti* to PPh_3), 4.21 (dd, J_{HH} = 12.7, J_{HP} = 7.8, =CH *syn* to PPh_3); $^{13}C\{^1H\}$ (ppm) 133.7 (d, J_{CP} = 10.0, *o*-PPh), 131.8 (s, *p*-PPh), 129.1 (d, J_{CP} = 10.7, *m*-PPh),[33] 141.1, 141.0, 128.9, 128.2, 127.3, 126.2, 122.8, 122.1 (8 s, 2C*Ph*), 101.1 (s, C_5H_5), 54.2 (d, J_{CP} = 5.4, =C *anti* to PPh_3), 50.5 (s, =C *syn* to PPh_3).

NMR Experiments. A. Homonuclear ^1H NOE difference spectra[19] were acquired at ambient probe temperature in $CDCl_3$, as reported earlier.[8] General procedures for dynamic NMR experiments[23a] have been described previously.[37] Near coalescence temperatures, spectra were acquired at 1–2 °C intervals after a 15-min thermal equilibration period. The T_1 values of the methyl protons of (*Z*)-**1a** were found to be 0.26–0.15 (−95 °C), 0.36–0.32 (−60 °C), and 0.48–0.44 s (−35 °C). **B.** 2D NMR spectra were recorded on a VXR-500 spectrometer with a $^1H/^{19}F$ probe. The 90° pulse width was determined to be 13.2 μs at −60 °C. The spectral width was 5734.8 Hz in both dimensions with 2048 points and acquisition time 0.179 s. The pulse delay was 1.321 s at −60 °C, and 1.821 s at −35 °C. Spectra were acquired with 512 increments and eight transients per increment. Quadrature data were acquired at each increment and Fourier transformed according to a literature procedure[38] to yield a hypercomplex spectrum.[22]

Crystal Structures. (*Z*)-1a·(CH_2Cl_2). Data were collected on a Syntex P$\bar{1}$ diffractometer as summarized in Table II. Cell constants were obtained from 35 reflections with 15° < 2θ < 25°. The space group was determined from systematic absences (*h0l* $h + l = 2n$, *0k0* $k = 2n$) and subsequent least-squares refinement. Lorentz, polarization, and empirical absorption (Ψ scans) corrections were applied. The structure was solved by the standard heavy-atom techniques with the SDP/VAX package.[39] Nonhydrogen atoms were refined with anisotropic thermal parameters. The =CHR hydrogens were located. Other hydrogen atom positions were calculated and added to the structure factor calculations but were not refined. Scattering factors, and Δ*f*′ and Δ*f*″ values, were taken from the literature.[40] **(*E*)-1a·(C_5H_{12})$_{0.5}$** (*RSS,SRR* diastereomer). Cell constants were obtained from 25 reflections with 17° < 2θ < 33°. The space group was determined from systematic absences (*hkl* $h + k = 2n$, *h0l* $h,l = 2n$) and subsequent least-squares refinement. The structure, including a severely disordered hemisolvate, was solved in an identical fashion.

Acknowledgment. We thank the NIH for support of this research.

Supplementary Material Available: Tables summarizing NMR decoupling experiments and anisotropic thermal parameters for (*Z*)-**1a**·(CH_2Cl_2) and (*E*)-**1a**·(C_5H_{12})$_{0.5}$ (3 pages). Ordering information is given on any current masthead page.

OM930036I

(37) (a) Buhro, W. E.; Zwick, B. D.; Georgiou, S.; Hutchinson, J. P.; Gladysz, J. A. *J. Am. Chem. Soc.* **1988**, *110*, 2427. (b) Zwick, B. D.; Dewey, M. A.; Knight, D. A.; Buhro, W. E.; Arif, A. M.; Gladysz, J. A. *Organometallics* **1992**, *11*, 2673.

(38) States, D. J.; Haberkorn, R. A.; Ruben, D. J. *J. Magn. Reson.* **1982**, *48*, 286.

(39) Frenz, B. A. The Enraf-Nonius CAD 4 SDP—A Real-time System for Concurrent X-ray Data Collection and Crystal Structure Determination. In *Computing and Crystallography*; Schenk, H.; Olthof-Hazelkamp, R.; van Konigsveld, H.; Bassi, G. C., Eds.; Delft University Press: Delft, Holland, 1978: pp 64–71.

(40) Cromer, D. T.; Waber, J. T. In *International Tables for X-ray Crystallography*; Ibers, J. A.; Hamilton, W. C., Eds.; Kynoch: Birmingham, England, 1974; Volume IV, pp 72–98, 149–150; tables 2.2B and 2.3.1.